BAW-1702

February 1982

ANALYSES OF CAPSULE RS1-B
SACRAMENTO MUNICIPAL UTILITY DISTRICT
RANCHO SECO UNIT 1

— Reactor Vessel Materials Surveillance Program —

Babcock & Wilcox
a McDermott company

77-1132121-00
BAW-1702
February 1982

ANALYSES OF CAPSULE RS1-B
SACRAMENTO MUNICIPAL UTILITY DISTRICT
RANCHO SECO UNIT 1

— Reactor Vessel Materials Surveillance Program —

by

A. L. Lowe, Jr., PE
W. A. Pavinich
W. L. Redd
J. K. Schmotzer
C. L. Whitmarsh

B&W Contract No. 582-7165-137

BABCOCK & WILCOX
Nuclear Power Group
Nuclear Power Generation Division
P. O. Box 1260
Lynchburg, Virginia 24505

Babcock & Wilcox

SUMMARY

This report describes the results of the examination of the first capsule of the Sacramento Municipal Utility District Rancho Seco Unit 1 reactor vessel surveillance program. The capsule was removed and examined after accumulating a fluence of 3.99×10^{18} nvt, which is equivalent to approximately 13 EFPY operation of the reactor vessel. The objective of the program is to monitor the effects of neutron irradiation on the tensile and fracture toughness properties of the reactor pressure vessel materials by the testing and evaluation of tension, Charpy impact, and compact fracture toughness specimens. The program was designed in accordance with the requirements of Appendix H to 10 CFR 50 and ASTM specification E185-73.

The capsule received an average fast fluence of 3.99×10^{18} n/cm^2 (E > 1 Mev) and the predicted fast fluence for the reactor vessel T/4 location at the end of the third cycle is 9.6×10^{17} n/cm^2 (E > 1 Mev). Based on the calculated fast flux at the vessel wall and an 80% load factor, the projected fast fluence that the Rancho Seco Unit 1 reactor pressure vessel will receive in 40 calendar years' operation is 1.62×10^{19} n/cm^2 (E > 1 Mev).

The results of the tensile tests indicated that the materials exhibited normal behavior relative to neutron fluence exposure. The Charpy impact data results exhibited the characteristic behavior of shift to higher temperature for both the 30 and 50 ft-lb transition temperatures as a result of neutron fluence damage and a decrease in upper shelf energy. These results demonstrated that the current techniques used for predicting the change in both the increase in the RT_{NDT} and the decrease in upper shelf properties due to irradiation are conservative. The compact fracture specimens were not tested at this time because no approved testing procedure was available. The results of these tests will be the subject of a separate report.

The recommended operating period was extended to 8 effective full power years as a result of the first capsule evaluation. These new operating limitations are in accordance with the requirements of Appendix G of 10 CFR 50.

CONTENTS

CONTENTS (Cont'd)

List of Tables

Tables (Cont'd)

List of Figures

1. INTRODUCTION

This report describes the results of the examination of the first capsule of the Sacramento Municipal Utility District Rancho Seco Unit 1 reactor vessel surveillance program. The capsule was removed and examined after the equivalent of three years of vessel operation.

The objective of the program is to monitor the effects of neutron irradiation of the tensile and impact properties of reactor pressure vessel materials under actual operating conditions. The surveillance program for Rancho Seco Unit 1 was designed and furnished by Babcock & Wilcox as described in BAW-10100A.[1] The program was designed in accordance with the requirements of Appendix H to 10 CFR Part 50 and ASTM specification E185-73 and was planned to monitor the effects of neutron irradiation on the reactor vessel material for the 40-year design life of the reactor pressure vessel. The future operating limitations established after the evaluation of the surveillance capsule are also in accordance with the requirement of 10 CFR 50, Appendixes G and H. The recommended operating period was extended to eight effective full power years as a result of the first capsule evaluation.

2. BACKGROUND

The ability of the reactor pressure vessel to resist fracture is the primary factor in ensuring the safety of the primary system in light water cooled reactors. The beltline region of the reactor vessel is the most critical region of the vessel because it is exposed to neutron irradiation. The general effects of fast neutron irradiation on the mechanical properties of such low-alloy ferritic steels as SA533, Grade B, used in the fabrication of the Rancho Seco Unit 1 reactor vessel are well characterized and documented in the literature. The low-alloy ferritic steels used in the beltline region of reactor vessels exhibit an increase in ultimate and yield strength properties with a corresponding decrease in ductility after irradiation. In reactor pressure vessel steels, the most serious mechanical property change is the increase in temperature for the transition from brittle to ductile fracture accompanied by a reduction in the upper shelf impact toughness.

Appendix G to 10 CFR 50, "Fracture Toughness Requirements," specifies minimum fracture toughness requirements for the ferritic materials of the pressure-retaining components of the reactor coolant pressure boundary (RCPB) of water-cooled power reactors and provides specific guidelines for determining the pressure-temperature limitations on operation of the RCPB. The toughness and operational requirements are specified to provide adequate safety margins during any condition of normal operation, including anticipated operational occurrences and system hydrostatic tests, to which the pressure boundary may be subjected over its service lifetime. Although the requirements of Appendix G to 10 CFR 50 became effective on August 13, 1973, the requirements are applicable to all boiling and pressurized water-cooled nuclear power reactors, including those under construction or in operation on the effective date.

Appendix H to 10 CFR 50, "Reactor Vessel Materials Surveillance Program Requirements," defines the material surveillance program required to monitor changes in the fracture toughness properties of ferritic materials in the reactor vessel beltline region of water-cooled reactors resulting from exposure to neutron irradiation and the thermal environment. Fracture toughness test data are obtained from material specimens withdrawn periodically from the reactor vessel. These data will permit determination of the conditions under which the vessel can be operated with adequate safety margins against fracture throughout its service life.

A method for guarding against brittle fracture in reactor pressure vessels is described in Appendix G to the ASME Boiler and Pressure Vessel Code, Section III. This method utilizes fracture mechanics concepts and the reference nil-ductility temperature, RT_{NDT}, which is defined as the greater of the drop weight nil-ductility transition temperature (per ASTM E-208) or the temperature that is 60F below that at which the material exhibits 50 ft-lb and 35 mils lateral expansion. The RT_{NDT} of a given material is used to index that material to a reference stress intensity factor curve (K_{IR} curve), which appears in Appendix G of ASME Section III. The K_{IR} curve is a lower bound of dynamic, static, and crack arrest fracture toughness results obtained from several heats of pressure vessel steel. When a given material is indexed to the K_{IR} curve, allowable stress intensity factors can be obtained for this material as a function of temperature. Allowable operating limits can then be determined using these allowable stress intensity factors.

The RT_{NDT} and, in turn, the operating limits of a nuclear power plant, can be adjusted to account for the effects of radiation on the properties of the reactor vessel materials. The radiation embrittlement and the resultant changes in mechanical properties of a given pressure vessel steel can be monitored by a surveillance program in which a surveillance capsule containing prepared specimens of the reactor vessel materials is periodically removed from the operating nuclear reactor and the specimens tested. The increase in the Charpy V-notch 50 ft-lb temperature, or the increase in the 35 mils of lateral expansion temperature, whichever results in the larger temperature shift due to irradiation, is added to the original RT_{NDT} to adjust it for radiation embrittlement. This adjusted RT_{NDT} is used to index the material to the K_{IR} curve, which, in turn is used to set operating limits for the nuclear power plant. These new limits take into account the effects of irradiation on the reactor vessel materials.

3. SURVEILLANCE PROGRAM DESCRIPTION

The surveillance program for Rancho Seco Unit 1 comprises six surveillance capsules designed to allow the owner to monitor the effects of neutron and thermal environment on the materials of the reactor pressure vessel core region. The capsules, which were inserted into the reactor vessel before initial plant startup, were positioned inside the reactor vessel between the thermal shield and the vessel wall at the locations shown in Figure 3-1. The six capsules, placed two in each holder tube, are positioned near the peak axial and azimuthal neutron flux. BAW-10100A includes a full description of capsule locations and design.[1] After the capsules are removed from Rancho Seco and included in the integrated reactor vessel materials surveillance program (RVSP), they are irradiated in the Davis-Besse Unit 1 reactor as described in BAW-1543.[2] During this period of irradiation capsule ANI-B was irradiated in site WZ as shown in Figure 3-2.

Capsule RS1-B was removed from Davis-Besse Unit 1 after cycle 1 and an accumulated fluence of approximately 4×10^{18} nvt. This capsule contained Charpy V-notch impact and tensile specimens fabricated of SA533, Grade B Class 1, weld metal, and weld metal compact fracture specimens. The specimens contained in the capsule are described in Table 3-1, and the chemistry and heat treatment of the surveillance material in capsule RS1-B are described in Table 3-2.

All test specimens were machined from the 1/4-thickness location of the plates. Charpy V-notch and tensile specimens from the vessel material were oriented with their longitudinal axes parallel to the principal rolling direction of the plate; specimens were also oriented transverse to the principal rolling direction. Capsule RS1-B contained dosimeter wires, described as follows:

Dosimeter wire	Shielding
U-Al alloy	Cd-Ag-alloy
Np-Al alloy	Cd-Ag-alloy
Nickel	Cd-Ag-alloy
0.56 wt % Co-Al alloy	Cd
0.56 wt % Co-Al alloy	None
Fe	None

Thermal monitors of low-melting eutectic alloys were included in the capsule. The eutectic alloys and their melting points are as follows:

Alloy	Melting point, F
90% Pb, 5% Ag, 5% Sn	558
97.5% Pb, 2.5% Ag	580
97.5% Pb, 1.5% Ag, 1.0% Sn	588
Lead	621
Cadmium	610

Table 3-1. Specimens in Surveillance Capsule RS1-B

	Number of test specimens		
Material description	Tension	CVN impact	1/2 T compact fracture[a]
Weld metal	2	12	8
Weld-HAZ Heat LL, transverse	—	12	—
Base metal Heat LL, transverse	2	12	--
Total per capsule	4	36	8

[a] Compact fracture specimens not pre-cracked.

Table 3-2. Chemistry and Heat Treatment of Surveillance Materials

Chemical Analysis

Element	Heat C-5062-1	Weld metal WF-193
C	0.20	0.065
Mn	1.26	1.50
P	0.013	0.016
S	0.017	0.008
Si	0.15	0.42
Ni	0.60	0.59
Mo	0.55	0.36
Cu	0.12	0.19

Heat Treatment

Heat No.	Temp, F	Time, h	Cooling
C-5062-1	1650-1700	9	Water quench
	1250	4.5	Air cooled
	1100-1150	60.0	Furnace cooled
WF-193	1100-1150	27.75	Furnace cooled

Figure 3-1. Reactor Vessel Cross Section Showing Surveillance Capsule Locations at Rancho Seco Unit 1

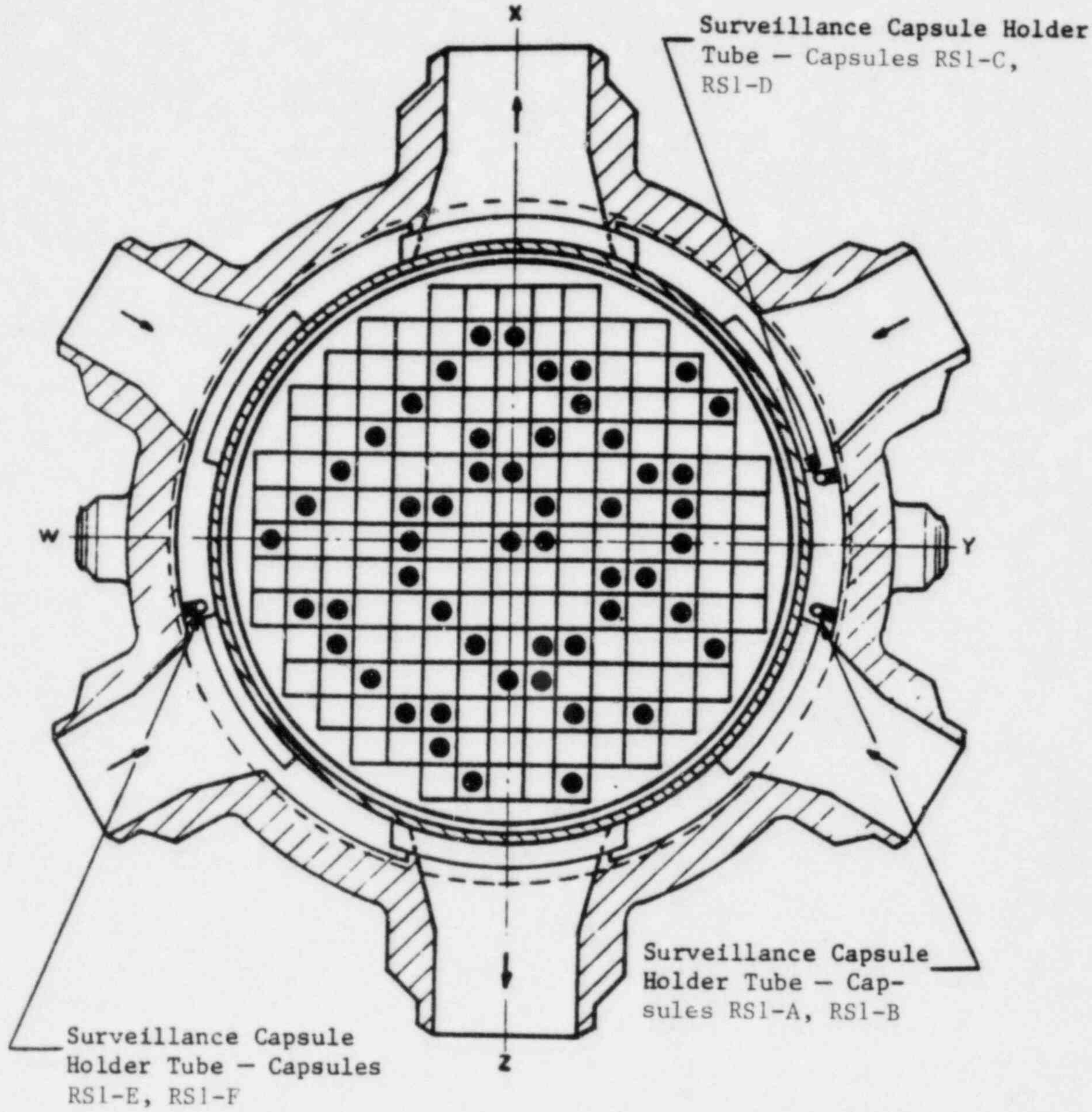

Figure 3-2. Reactor Vessel Cross Section Showing Location of Rancho Seco Unit 1 Capsule in Davis-Besse Unit 1 Reactor

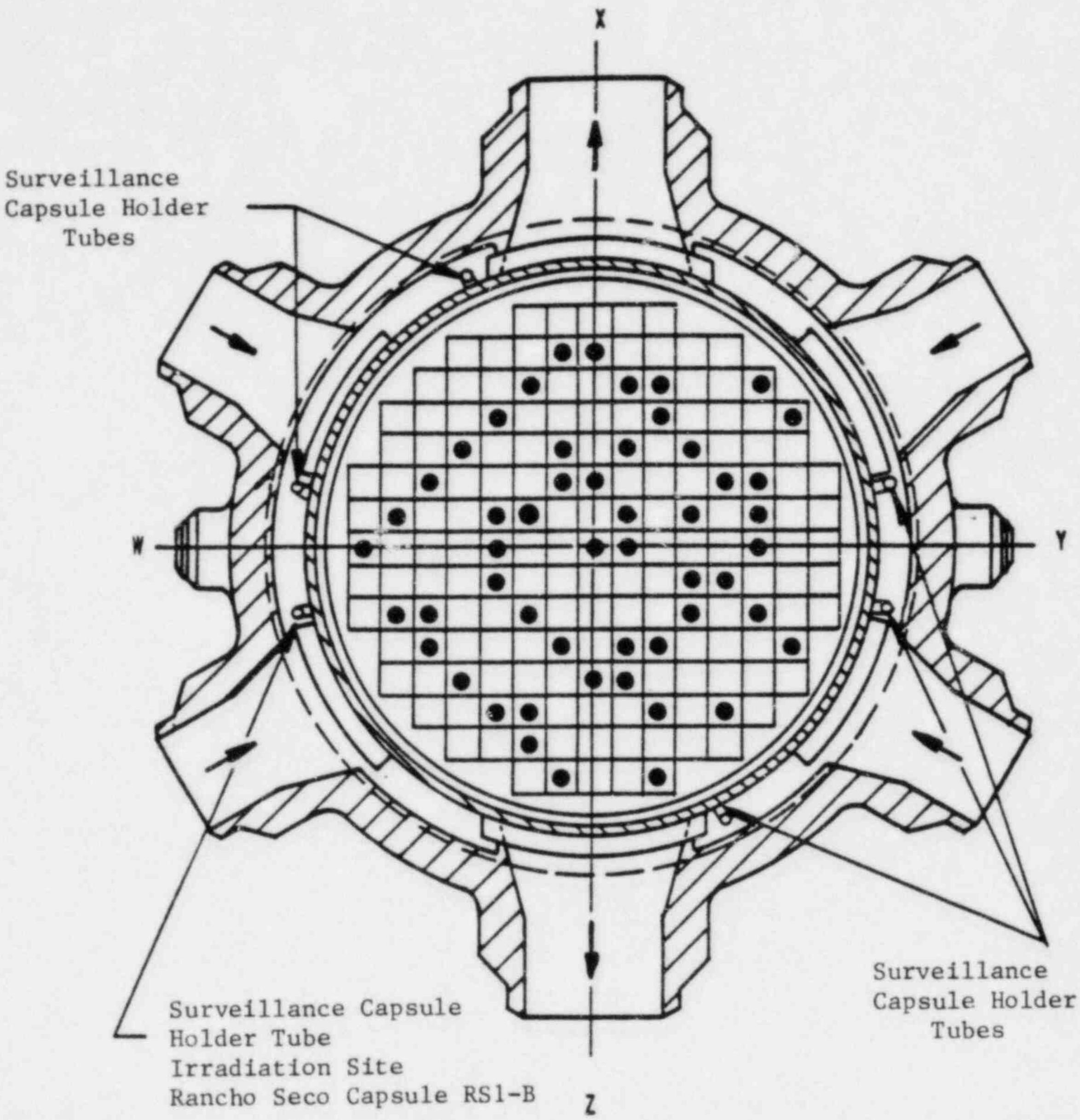

4. PREIRRADIATION TESTS

Unirradiated material was evaluated for two purposes: (1) to establish a baseline of data to which irradiated properties data could be referenced, and (2) to determine those materials properties to the extent practical from available material, as required for compliance with Appendixes G and H to 10 CFR 50.

4.1. Tensile Tests

Tensile specimens were fabricated from the reactor vessel shell course plate and weld metal. The subsize specimens were 4.25 inches long with a reduced section 1.750 inches long by 0.357 inch in diameter. They were tested on a 55,000-lb-load capacity universal test machine at a crosshead speed of 0.050 inch per minute. A 4-pole extension device with a strain gaged extensometer was used to determine the 0.2% yield point. Test conditions were in accordance with the applicable requirements of ASTM A370-72. For each material type and/or condition, six specimens in groups of three were tested at both room temperature and 580F. The tension-compression load cell used had a certified accuracy of better than ±0.5% of full scale (25,000 lb). All test data for the preirradiation tensile specimens are given in Appendix B.

4.2. Impact Tests

Charpy V-notch impact tests were conducted in accordance with the requirements of ASTM Standard Methods A370-72 and E23-72 on an impact tester certified to meet Watertown standards. Test specimens were of the Charpy V-notch type, which were nominally 0.394 inch square and 2.165 inches long.

Prior to testing, specimens were temperature-controlled in liquid immersion baths, capable of covering the temperature range from -85 to +550F. Specimens were removed from the baths and positioned in the test frame anvil with tongs specifically designed for the purpose. The pendulum (hammer) was released manually, allowing the specimens to be broken within 5 seconds from their removal from the temperature baths.

Impact test data for the unirradiated baseline reference materials are presented in Appendix C. Tables C-1 through C-3 contain the basis data which are plotted in Figures C-1 through C-3.

4.3. Compact Fracture Tests

The compact fracture specimens fabricated from the weld metal, which were a part of the capsule specimen inventory, were not tested because of the lack of a recognized testing procedure. These specimens will be kept in bonded storage until an acceptable test procedure is developed. The results of the testing of these specimens will be the subject of a separate report.

5. POSTIRRADIATION TESTS

5.1. Thermal Monitors

Surveillance capsule ANI-B contained three temperature monitor holder tubes, each containing five fusible alloys with different melting points ranging from 558 to 621F. All the thermal monitors at 558, 580, and 588F had melted, while these at the 610F location also showed no change; however, the monitor at 621F appeared to have melted at two of three locations, and another showed slumping. It is safe to assume that the monitors were placed in the wrong locations in the holder tubes. From these data it was concluded that the irradiated specimens had been exposed to a maximum temperature in the range of 588 to 610F during the reactor vessel operating period. There appeared to be no significant temperature gradient along the capsule length.

5.2. Tensile Test Results

The results of the post-irradiation tensile tests are presented in Table 5-1. Tests were performed on specimens at both room temperature and 580F using the same test procedures and techniques used to test the unirradiated specimens (section 4.1). In general, the ultimate strength and yield strength of the material increased slightly with a corresponding slight decrease in ductility; both effects were the result of neutron radiation damage. The type of behavior observed and the degree to which the material properties changed is within the range of changes to be expected for the radiation environment to which the specimens were exposed.

The results of the preirradiation tensile tests are presented in Appendix B.

5.3. Charpy V-Notch Impact Test Results

The test results from the irradiated Charpy V-notch specimens of the reactor vessel beltline material and the correlation monitor material are presented in Tables 5-2 through 5-4 and Figures 5-1 through 5-3. The test procedures and techniques were the same as those used to test the unirradiated specimens (section 4.2). The data show that the material exhibited a sensitivity to irradiation within the values predicted from its chemical composition and the fluence to which it was exposed.

The results of the preirradiation Charpy V-notch impact tests are given in Appendix C.

Table 5-1. Tensile Properties of Capsule RS1-B Base Metal and Weld Metal Irradiated to 3.99E18 n/cm^2 (>1 Mev)

Specimen No.	Test temp, F	Strength, psi		Elongation, %		Red'n in area, %
		Yield	Ult.	Unif	Total	
Base Metal, Transverse						
LL-618	69	69,400	90,600	17	30	62
LL-602	582	81,900	85,600	15	23	57
Weld Metal						
MM-005	69	86,900	103,100	15	26	57
MM-007	579	75,600	92,500	12	18	47

Table 5-2. Charpy Impact Data From Capsule RS1-B Base Metal Irradiated to 3.99E18 n/cm^2 (>1 Mev)

Specimen No.	Test temp, F	Absorbed energy, ft-lb	Lateral expansion, 10^{-3} in.	Shear fracture, %
LL-686	0	13.5	15.0	0
LL-651	38	30.5	28.5	10
LL-688	58	44.5	40.0	20
LL-652	75	47.0	45.0	15
LL-692	75	50.0	48.0	35
LL-707	75	53.0	44.5	25
LL-673	95	42.5	42.0	30
LL-626	110	61.5	57.0	40
LL-706	145	74.5	64.5	100
LL-664	145	87.5	70.0	100
LL-618	228	89.0	75.0	100
LL-691	280	88.5	77.5	100

Table 5-3. Charpy Impact Data From Capsule RS1-B Heat-Affected Zone Metal Irradiated to 3.99E18 n/cm^2 (>1 Mev)

Specimen No.	Test temp, F	Absorbed energy, ft-lb	Lateral expansion, 10^{-3} in.	Shear fracture, %
LL-391	-80	26.0	17.0	10
LL-308	-58	31.5	23.0	15
LL-350	-35	15.5	12.0	5
LL-317	-22	39.5	28.0	25
LL-371	0	44.0	38.5	65
LL-389	19	58.5	50.0	70
LL-333	38	74.0	56.0	100
LL-355	75	67.5	55.5	90
LL-358	110	66.0	58.5	70
LL-302	145	78.0	75.0	100
LL-330	193	71.5	64.0	100
LL-390	241	98.0	76.0	100

Table 5-4. Charpy Impact Data From Capsule RS1-B Weld Metal Irradiated to 3.99E18 n/cm^2 (>1 Mev)

Specimen No.	Test temp, F	Absorbed energy, ft-lb	Lateral expansion, 10^{-3} in.	Shear fracture, %
MM-089	0	11.5	7.5	0
MM-053	38	17.0	18.0	20
MM-070	75	28.5	26.5	25
MM-075	110	32.0	31.0	45
MM-017	145	34.0	32.0	35
MM-016	194	46.5	52.5	98
MM-050	228	50.0	48.0	100
MM-058	280	51.0	52.5	100
MM-004	342	51.5	54.0	100
MM-080	578	40.5	42.5	100

Figure 5-1. Charpy Impact Data for Irradiated Base Metal, Transverse Direction

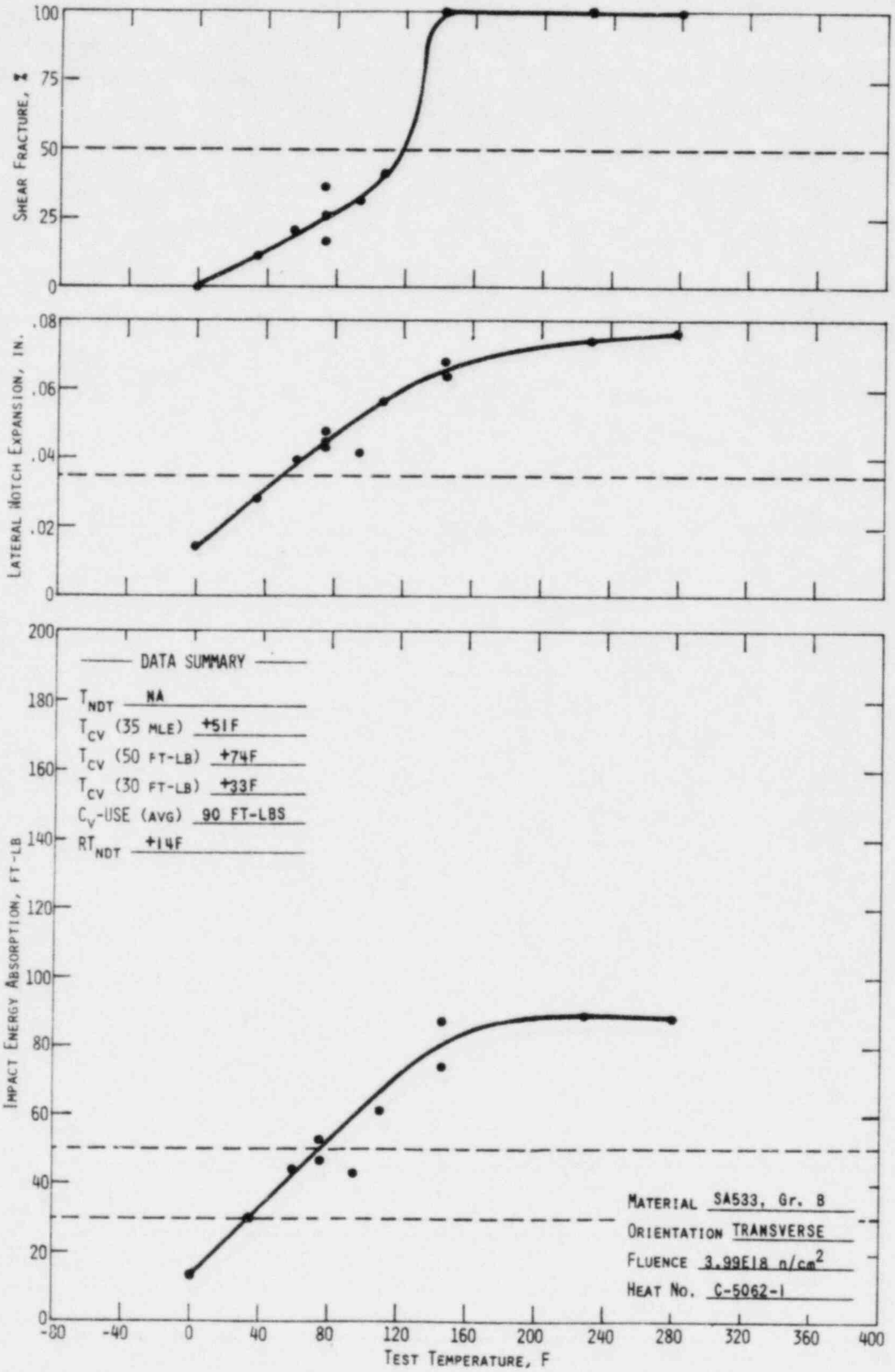

Figure 5-2. Charpy Impact Data for Irradiated Base Metal, Heat-Affected Zone

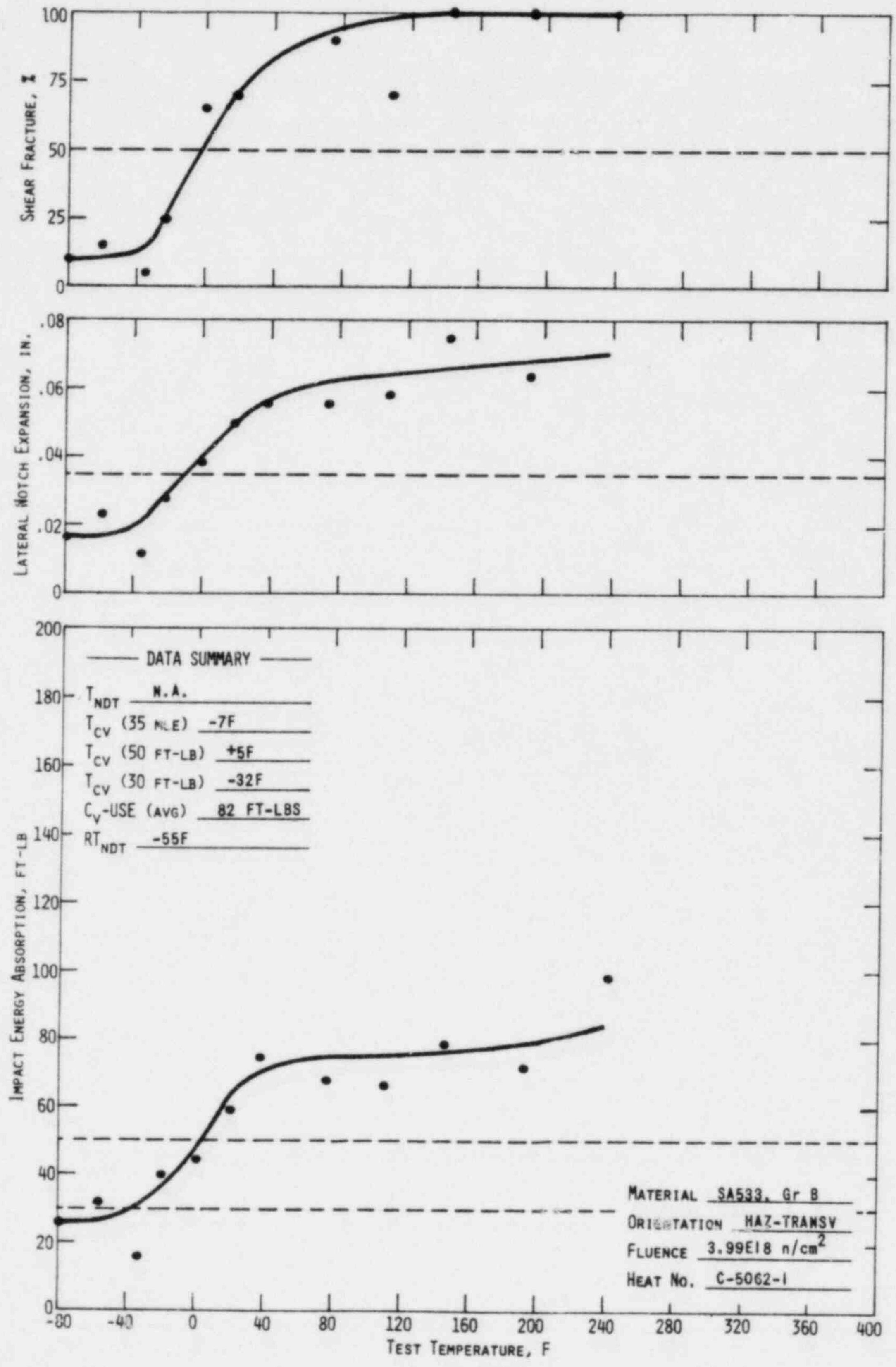

Figure 5-3. Charpy Impact Data for Irradiated Weld Metal

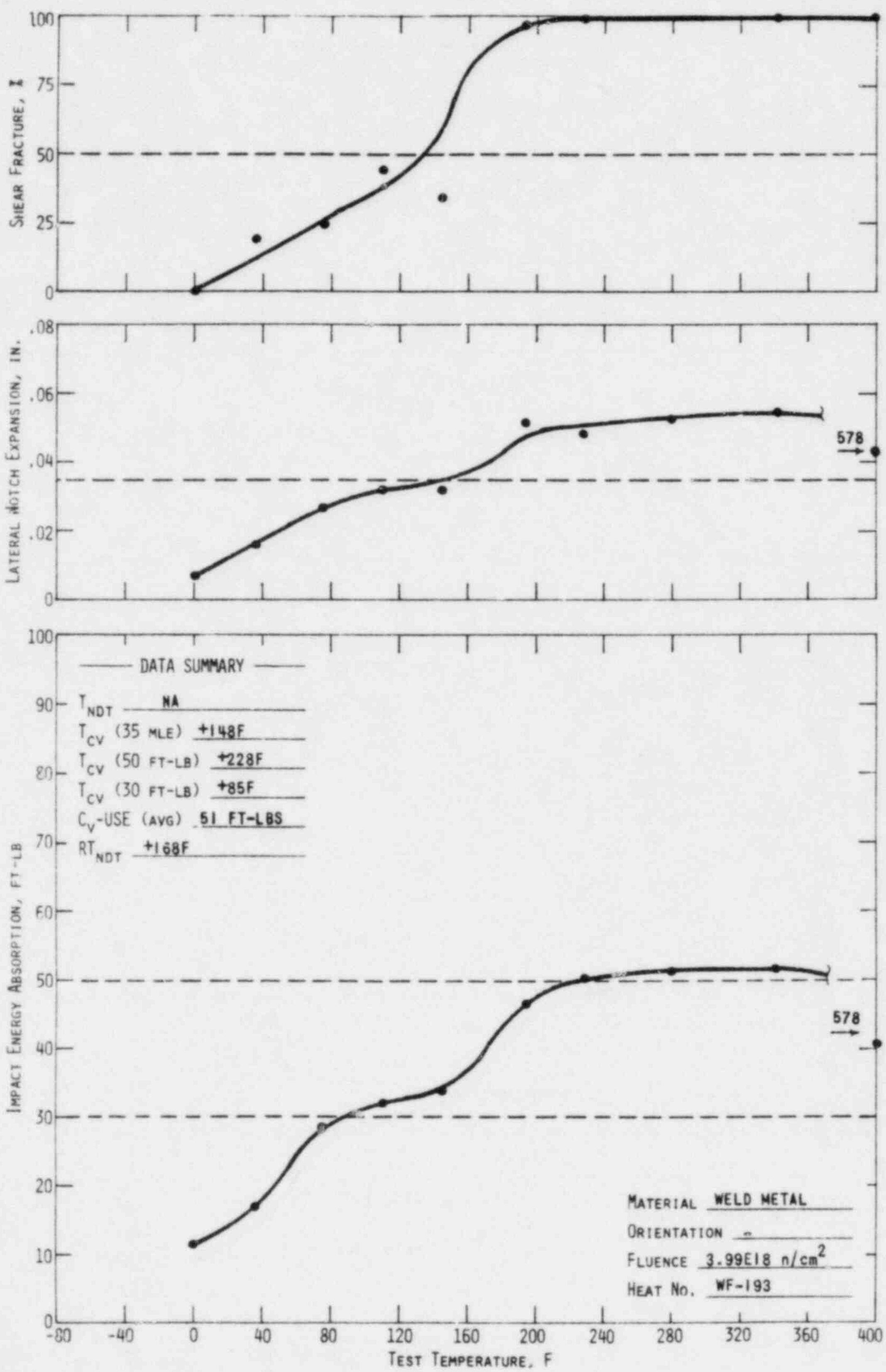

6. NEUTRON DOSIMETRY

6.1. Background

Fluence analysis as a part of the pressure vessel surveillance program has three objectives, (1) determination of maximum fluence at the pressure vessel as a function of reactor operation, (2) prediction of pressure vessel fluence in the future, and (3) determination of the test specimen fluence within the surveillance capsule. Vessel fluence data are used to evaluate changes in reference transition temperature and upper shelf energy levels, and to establish pressure-temperature operation curves. Test specimen fluence data are used to establish a correlation between changes in material properties and fluence exposure. Fluence data are obtained from flux distributions calculated with a computer model of the reactor. The accuracy of calculated fast flux is enhanced by the use of a normalization factor which utilizes measured activity data obtained from capsule dosimeters.

A significant aspect of the surveillance program is to provide a correlation between the neutron fluence above 1 Mev and the radiation-induced property changes noted in the surveillance specimens. To permit such a correlation, activation detectors with reaction thresholds in the energy range of interest were placed in each surveillance capsule. The properties of interest for the detectors are given in Tables 6-1 and E-1.

Because of a long half-life (30 years) and effective threshold energies of 0.5 and 1.1 Mev, the measurements of ^{137}Cs production from fission reactions in ^{237}Np (and ^{238}U) are more directly applicable to analytical determinations of the fast neutron fluence (E > 1 Mev) for multiple fuel cycles than are other dosimeter reactions. Other dosimeter reactions are useful as corroborating data for shorter time intervals and/or higher energy fluxes. Short-lived isotope activities are representative of reactor conditions only over the latter portion of the irradiation period (fuel cycle), whereas reactions with a threshold energy higher than 2 or 3 Mev do not record a significant part of the total fast flux.

The energy-dependent neutron flux is not directly available from activation detectors because the dosimeters register only the integrated effect of the neutron flux on the target material as a function of both irradiation time and neutron energy. To obtain an accurate estimate of the average neutron flux incident upon the detector, the following parameters must be known: the operating history of the reactor, the energy response of the given detector, and the neutron spectrum at the detector location. Of these parameters, the definition of the neutron spectrum is the most difficult to obtain. Essentially, two means are available to obtain it: iterative unfolding of experimental dosimeter data and/or analytical methods. Due to a lack of sufficient threshold reaction detectors satisfying both the threshold energy and half-life requirements of a surveillance program, calculated spectra are used in this analysis.

Neutron transport calculations in two-dimensional geometry are used to calculate energy-dependent flux distributions throughout the reactor. Reactor conditions are selected to be representative of an average over the irradiation time period. Geometric details are selected to explicitly represent the surveillance capsule assembly and the pressure vessel. The detailed calculational procedure is described in Appendix D.

6.2. Vessel Fluence

The maximum fluence (E > 1.0 Mev) in the pressure vessel through cycle 3 was determined to be 1.73 (+17) n/cm^2 based on an average neutron flux of 1.94 (+10) n/cm^2-s (Tables 6-2 and 6-3). The location of maximum fluence is a point at the cladding/vessel interface at an elevation about 110 cm above the lower active fuel boundary and an azimuthal (peripheral) location of 12° from a major axis (across flats diameter). Fluence data have been extrapolated to 32 EFPY of operation based on the premise that ex-core flux is proportional to fast flux that escapes the reactor core (Appendix D). Core escape flux values are available from fuel management analyses of future fuel cycles.

Relative fluence as a function of radial location in the pressure vessel is shown in Figure 6-1. Pressure vessel lead factors (clad interface flux/in-vessel flux) for the T/4, T/2, 3T/4 locations are 1.8, 3.7, and 7.7, respectively. Relative fluence as a function of azimuthal angle is shown in Figure 6-2. A peak occurs at about 12° which roughly corresponds to a corner of the core (also to four symmetric capsule locations, including capsule RS1-B). Two other capsule locations correspond to the azimuthal minimum at about 27°. However, it should be noted that the maximum:minimum flux ratio is only 1.4. Fast neutron flux is increased by approximately 1.25 in the capsule due to differences in scattering and absorption cross sections between steel and water.

6.3. Capsule Fluence

Fast fluence at the center of the surveillance capsule was calculated to be 3.99 (+18) n/cm^2, 13% of which occurred in Rancho Seco and 87% in Davis Besse (Table 6-4). These data represent average values in the capsule. In Rancho Seco, capsule RS1-B was located in a lower holder tube position 11° off axis and approximately 211 cm from the core center for 170.5 EFPD. It was then inserted in Davis Besse in a lower holder tube position 11° off axis and 202 cm from the core center for an additional 374 EFPD. During the latter irradiation period, the capsule was estimated to have been rotated 20° counterclockwise relative to its original design orientation (keyway facing the reactor core).

Table 6-1. Surveillance Capsule Detectors

Detector reaction	Effective lower energy limit, Mev	Isotope half-life
$^{54}Fe(n,p)^{54}Mn$	2.5	312.5 days
$^{58}Ni(n,p)^{58}Co$	2.3	70.85 days
$^{238}U(n,f)^{137}Cs$	1.1	30.03 years
$^{237}Np(n,f)^{137}Cs$	0.5	30.03 years

Table 6-2. Pressure Vessel Flux

	Fast flux, n/cm^2-s (E > 1 Mev)			Flux, n/cm^2-s (E > 0.1 Mev), inside surface (max location)
	Inside surface (max location)	T/4	3T/4	
Cycle 1-3, 1029.5 EFPD	1.94(+10)	1.1(+10)	2.5(+9)	4.2(+10)

Table 6-3. Pressure Vessel Fluence Gradient

	Fast fluence, n/cm^2 (E > 1.0 Mev)		
Cumulative irradiation time	Inside surface (max location)	T/4	3T/4
End of cycle 3 (1029.5 EFPD)	1.73(+18)	9.6(+17)	2.2(+17)
8 EFPY	4.35(+18)	2.4(+18)	5.7(+17)
32 EFPY	1.62(+19)	9.0(+18)	2.1(+18)

Table 6-4. Surveillance Capsule Fluence

	Flux, n/cm^2-s (E > 1 Mev)	Fluence, n/cm^2	Cumulative fluence, n/cm^2	Flux, n/cm^2-s (E > 0.1 Mev)
RS-1, cycle 1A, 170.5 EFPD	3.59(+10)	5.29(+17)	5.29(+17)	7.31(+10)
DB-1, cycle 1, 374 EFPD	1.07(+11)	3.46(+18)	3.99(+18)	2.52(+11)

Figure 6-1. Flux (E > 1 Mev) Gradient Radially Through Pressure Vessel for Rancho Seco Cycles 1 Through 3

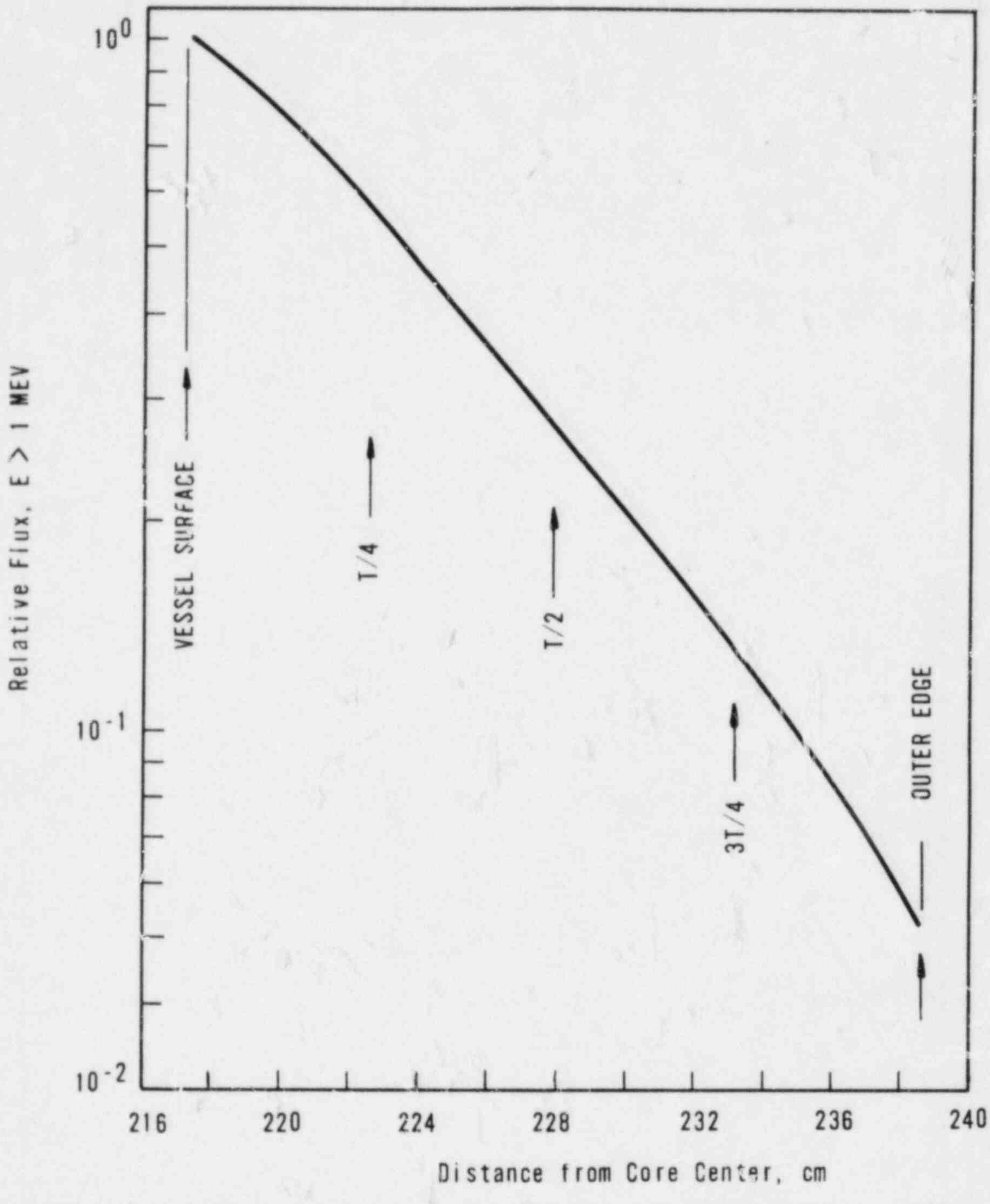

Figure 6-2. Azimuthal Fluence Gradient (E > 1 Mev) at Inside Surface of Pressure Vessel in Rancho Seco for Cycles 1 Through 3

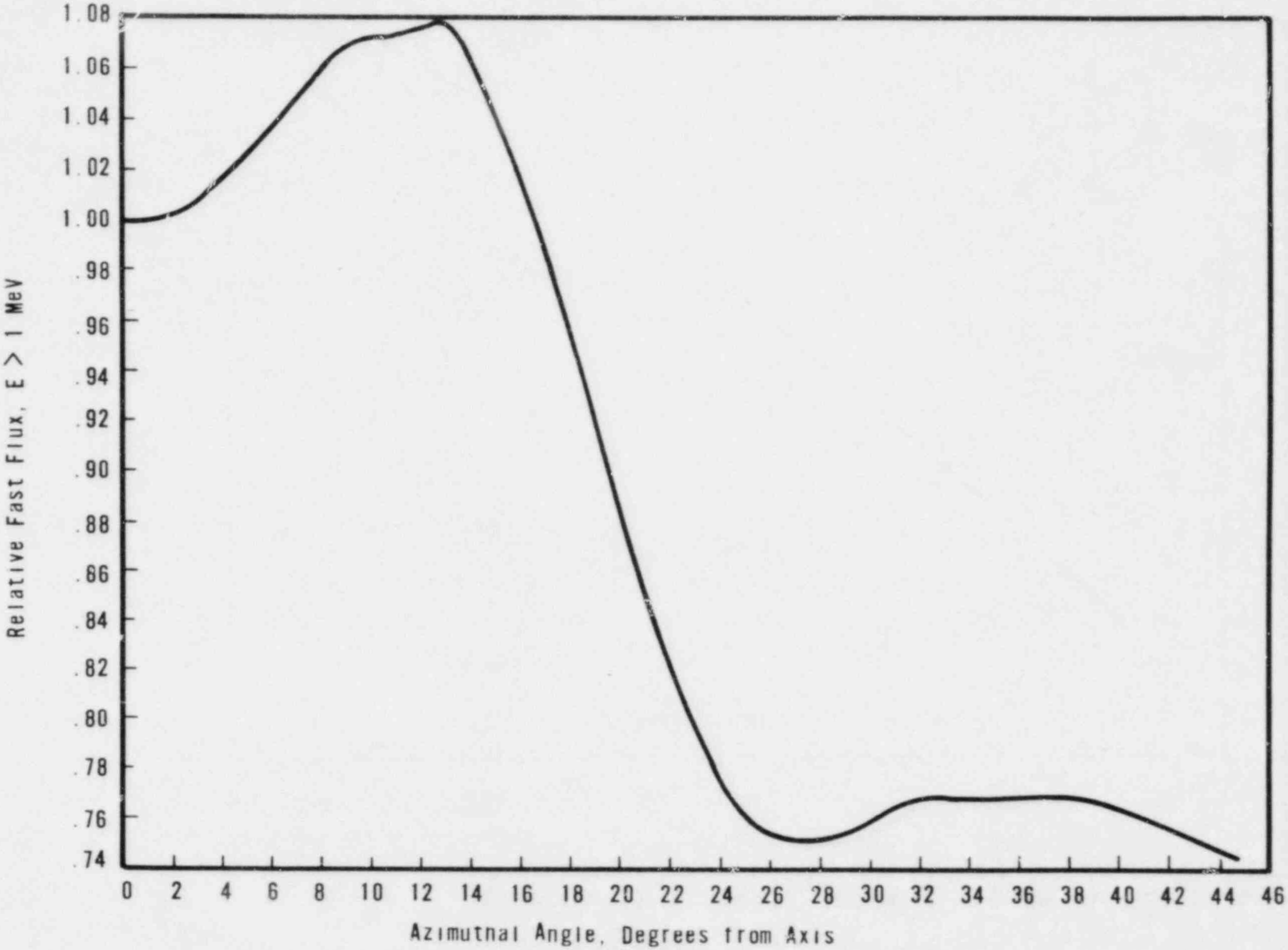

7. DISCUSSION OF CAPSULE RESULTS

7.1. Preirradiation Property Data

A review of the unirradiated properties of the reactor vessel core belt region indicated no significant deviation from expected properties except in the case of the upper shelf properties of the weld metal. Based on the predicted end-of-service peak neutron fluence value at the 1/4T vessel wall location and the copper content of the weld metals, it is predicted that the end-of-service Charpy upper shelf energys (USE) will be below 50 ft-lb. The weld metal selected for inclusion in the · irveillance program was selected in accordance with the criteria in effect at the time the program was designed for Rancho Seco Unit 1. The applicable selection criterion was based on the unirradiated properties only and before it was known that the weld metals are more sensitive to radiation damage than the base metal. The inclusion of compact fracture specimens was an effort to correct the program's deficiency and update to more current requirements.

7.2. Irradiated Property Data

7.2.1. Tensile Properties

Table 7-1 compares irradiated and unirradiated tensile properties. At both room temperature and elevated temperature, the ultimate and yield strength changes in the base metal as a result of irradiation and the corresponding changes in ductility are negligible. There appears to be some strengthening, as indicated by increases in ultimate and yield strength and similar decreases in ductility properties. All changes observed in the base metal are such as to be considered within acceptable limits. The changes at both room temperature and 580F in the properties of the weld metal are greater than those observed for the base metal, indicating a greater sensitivity of the weld metal to irradiation damage. In either case, the changes in tensile properties are insignificant relative to the analysis of the react ,r vessel materials at this period in service life.

7. DISCUSSION OF CAPSULE RESULTS

7.1. Preirradiation Property Data

A review of the unirradiated properties of the reactor vessel core belt region indicated no significant deviation from expected properties except in the case of the upper shelf properties of the weld metal. Based on the predicted end-of-service peak neutron fluence value at the 1/4T vessel wall location and the copper content of the weld metals, it is predicted that the end-of-service Charpy upper shelf energys (USE) will be below 50 ft-lb. The weld metal selected for inclusion in the surveillance program was selected in accordance with the criteria in effect at the time the program was designed for Rancho Seco Unit 1. The applicable selection criterion was based on the unirradiated properties only and before it was known that the weld metals are more sensitive to radiation damage than the base metal. The inclusion of compact fracture specimens was an effort to correct the program's deficiency and update to more current requirements.

7.2. Irradiated Property Data

7.2.1. Tensile Properties

Table 7-1 compares irradiated and unirradiated tensile properties. At both room temperature and elevated temperature, the ultimate and yield strength changes in the base metal as a result of irradiation and the corresponding changes in ductility are negligible. There appears to be some strengthening, as indicated by increases in ultimate and yield strength and similar decreases in ductility properties. All changes observed in the base metal are such as to be considered within acceptable limits. The changes at both room temperature and 580F in the properties of the weld metal are greater than those observed for the base metal, indicating a greater sensitivity of the weld metal to irradiation damage. In either case, the changes in tensile properties are insignificant relative to the analysis of the reactor vessel materials at this period in service life.

7.2.2. Impact Properties

The behavior of the Charpy V-notch impact data is more significant to the calculation of the reactor system's operating limitations. Table 7-2 compares the observed changes in irradiated Charpy impact properties with the predicted changes as shown in Figures 7-1 through 7-3.

The 50 ft-lb transition temperature shift for the base metal is not in good agreement with the shift that would be predicted according to Regulatory Guide 1.99. The less-than-ideal comparison may be attributed to the spread in the data of the unirradiated material combined with a minimum of data points to establish the irradiated curve. Under these conditions, the comparison indicates that the estimating curves in RG 1.99 for medium-copper materials and at low fluence levels are reasonably accurate for predicting the 50-ft-lb transition temperature shifts.

The 30 ft-lb transition temperature shift for the base metal is not in as good agreement with the value predicted according to Regulatory Guide 1.99, although it would be expected that these values would exhibit better comparison when it is considered that a major portion of the data used to develop Regulatory Guide 1.99 was taken at the 30 ft-lb temperature.

The increase in the 35-mil lateral expansion transition temperature is compared with the shift in RT_{NDT} curve data in a manner similar to the comparison made for the 50 ft-lb transition temperature shift. These data show a behavior similar to that observed from the comparison of the observed and predicted 50 ft-lb transition data.

All the transition temperature measurements for the weld metal are in poor agreement with the predicted shift. This can be attributed to the chemistry of the weld metal as compared to the nominal chemistry of normal weld metal for which the prediction curves were developed. This being the case, it would not be expected that the current prediction techniques will apply to the weld metal.

The data for the decrease in Charpy USE with irradiation showed a poor agreement with predicted values for both the base metal and the weld metal. However, the poor comparison of the measured data with the predicted value is not unexpected in view of the lack of data for medium- to high-copper-content materials at low to medium fluence values that were used to develop the estimating curves.

Results from other capsules indicate that the RT_{NDT} estimating curves have greater inaccuracies at the low neutron fluence levels ($\leq 1 \times 10^{18}$ n/cm^2). This inaccuracy is attributed to the limited data at the low fluence values and of the fact that the majority of the data used to define the curves in RG 1.99 are based on the shift at 30 ft-lb as compared to the current requirement of 50 ft-lb. For most materials the shifts measured at 50 ft-lb/35 MLE are expected to be higher than those measured at 30 ft-lb. The significance of the shifts at 50 ft-lb and/or 35 MLE is not well understood at present, especially for materials having USEs that approach the 50 ft-lb level and/or the 35 MLE level. Materials with this characteristic may have to be evaluated at transition energy levels lower than 50 ft-lb.

The design curves for predicting the shift at 50 ft-lb/35 MLE will probably be modified as data become available; until that time, the design curves for predicting the RT_{NDT} shift as given in Regulatory Guide 1.99 are considered adequate for predicting the RT_{NDT} shift of those materials for which data are not available and will continue to be used to establish the pressure-temperature operational limitations for the irradiated portions of the reactor vessel.

The lack of good agreement of the change in Charpy USE is further support of the inaccuracy of the predictio. curves at the lower fluence levels. Although the prediction curves are conservative in that they predict a larger drop in upper shelf than is observed for a given fluence and copper content, the conservatism can unduly restrict the operational limitations. These data support the contention that the USE drop curves will have to be modified as more reliable data become available; until that time the design curves used to predict the decrease in USE are conservative.

Table 7-1. Comparison of Tensile Test Results

	Room temp test		Elevated temp test (580F)	
	Unirr	Irrad	Unirr	Irrad
Base Metal — C-5062-1 Transverse				
Fluence, 10^{18} n/cm^2 (> 1 Mev)	0	3.99	0	3.99
Ult tensile strength, ksi	83.8	90.6	82.9	85.6
0.2% yield strength, ksi	63.9	69.4	57.5	61.9
Uniform elongation, %	16	17	18	15
Total elongation, %	27	30	24	23
RA, %	66	62	57	57
Weld Metal — WF-193				
Fluence, 10^{18} n/cm^2 (> 1 Mev)	0	3.99	0	3.99
Ult tensile strength, ksi	83.5	103.1	80.6	92.5
0.2% yield strength, ksi	67.5	86.9	61.6	75.6
Uniform elongation, %	16	15	14	12
Total elongation, %	29	26	21	18
RA, %	63	57	52	47

Table 7-2. Observed Vs Predicted Changes in Irradiated Charpy Impact Properties

Material	Observed	Predicted[a]
Increase in 30-ft-lb trans temp, F		
Base material (C-5062-1) Transverse	29	66
Heat-affected zone (C-5062-1)	20	66
Weld metal (WF-193)	99	120
Increase in 50-ft-lb trans temp, F		
Base material (C-5062-1) Transverse	29	66
Heat-affected zone (C-5062-1)	24	66
Weld metal (WF-193)	192	120
Increase in 35-MLE trans temp, F		
Base material (C-5062-1) Transverse	30	66[b]
Heat-affected zone (C-5062-1)	29	66[b]
Weld metal (WF-193)	153	120[b]
Decrease in Charpy USE, ft-lb		
Base material (C-5062-1) Transverse	0	12
Heat-affected zone (C-5062-1)	14	13
Weld metal (WF-193)	7	14

[a] These values predicted per Regulatory Guide 1.99, Revision 1.

[b] Based on the assumption that MLE as well as 50 ft-lb transition temperature is used to control the shift in RT_{NDT}.

8. DETERMINATION OF RCPB PRESSURE-TEMPERATURE LIMITS

The pressure-temperature limits of the reactor coolant pressure boundary (RCPB) of Rancho Seco Unit 1 are established in accordance with the requirements of 10 CFR 50, Appendix G. The methods and criteria employed to establish operating pressure and temperature limits are described in topical report BAW-10046.[3] The objective of these limits is to prevent nonductile failure during any normal operating condition, including anticipated operation occurrences and system hydrostatic tests. The loading conditions of interest include the following:

1. Normal operations, including heatup and cooldown.
2. Inservice leak and hydrostatic tests.
3. Reactor core operation.

The major components of the RCPB have been analyzed in accordance with 10 CFR 50, Appendix G. The closure head region, the reactor vessel outlet nozzle, and the beltline region have been identified as the only regions of the reactor vessel, and consequently of the RCPB, that regulate the pressure-temperature limits. Since the closure head region is significantly stressed at relatively low temperatures (due to mechanical loads resulting from bolt preload), this region largely controls the pressure-temperature limits of the first several service periods. The reactor vessel outlet nozzle also affects the pressure-temperature limit curves of the first several service periods. This is due to the high local stresses at the inside corner of the nozzle, which can be two to three times the membrane stresses of the shell. After the first several years of neutron radiation exposure, the RT_{NDT} of the beltline region materials will be high enough that the beltline region of the reactor vessel will start to control the pressure-temperature limits of the RCPB. For the service period for which the limit curves are established, the maximum allowable pressure as a function of fluid temperature is obtained through a point-by-point comparison of the limits imposed by the closure head region, the outlet nozzle, and the beltline region. The maximum allowable pressure is taken to be the lowest of three calculated pressures.

The limit curves for Rancho Seco Unit 1 are based on the predicted values of the adjusted reference temperatures of all the beltline region materials at the end of the eighth full-power year. The eighth full-power year was selected because it is estimated that the second surveillance capsule will be withdrawn at the end of the refueling cycle when the estimated fluence corresponds to approximately the ninth full-power year. The time difference between the withdrawal of the first and second surveillance capsule provides adequate time for re-establishing the operating pressure and temperature limits for the period of operation between the second and third surveillance capsule withdrawals.

The unirradiated impact properties were determined for the surveillance beltline region materials in accordance with 10 CFR 50, Appendixes G and H. For the other beltline region and RCPB materials for which the measured properties are not available, the unirradiated impact properties and residual elements, as originally established for the beltline region materials, are listed in Table A-1. The adjusted reference temperatures are calculated by adding the predicted radiation-induced ΔRT_{NDT} and the unirradiated RT_{NDT}. The predicted ΔRT_{NDT} is calculated using the respective neutron fluence and copper and phosphorus contents. Figure 8-1 illustrates the calculated peak neutron fluence at several locations through the reactor vessel beltline region wall and at the center of the surveillance capsules at each of two locations as a function of exposure time. The supporting information for Figure 8-1 is described in BAW-10100.[1] The neutron fluence values of Figure 8-1 are the predicted fluences, which have been demonstrated (section 6) to be conservative. The design curves of Regulatory Guide 1.99* were used to predict the radiation-induced ΔRT_{NDT} values as a function of the material's copper and phosphorus content and neutron fluence.

The neutron fluences and adjusted RT_{NDT} values of the beltline region materials at the end of the eighth full-power year are listed in Table 8-1. The neutron fluences and adjusted RT_{NDT} values are given for the 1/4T and 3/4T vessel wall locations (T = wall thickness). The assumed RT_{NDT} of the closure head region and the outlet nozzle steel forgings is 60F, in accordance with BAW-10046P).[3]

*Revision 1, January 1976.

Figure 8-2 shows the reactor vessel's pressure-temperature limit curve for normal heatup. This figure also shows the core criticality limits as required by 10 CFR 50, Appendix G. Figure 8-3 and 8-4 show the vessel's pressure-temperature limit curve for normal cooldown and for heatup during inservice leak and hydrostatic tests, respectively. All pressure-temperature limit curves are applicable up to the ninth effective full-power year. Protection against nonductile failure is ensured by maintaining the coolant pressure below the upper limits of the pressure-temperature limit curves. The acceptable pressure and temperature combinations for reactor vessel operation are below and to the right of the limit curve. The reactor is not permitted to go critical until the pressure-temperature combinations are to the right of the criticality limit curve. To establish the pressure-temperature limits for protection against nonductile failure of the RCPB, the limits presented in Figures 8-2 through 8-4 must be adjusted by the pressure differential between the point of system pressure measurement and the pressure on the reactor vessel controlling the limit curves. This is necessary because the reactor vessel is the most limiting component of the RCPB.

Table 8-1. Data for Preparation of Pressure-Temperature Limit Curves for Rancho Seco — Applicable Through Eighth Full Power Year

Material ident			Weldment location				Chemistry		Neutron fluence at end of 8 EFPY (E > 1 Mev) n/cm^2		Radiation-induced ΔRT_{NDT} at end of 8 EFPY, F(a)		Adjusted RT_{NDT} at end of 8 EFPY, F	
Heat No.	Type	Beltline region location	Core midplane to weld CL, cm	Location from major axis, degrees	Weld 1/4T location	Unirr RT_{NDT}, F	Copper content, %	Phosphorus content, %	At 1/4T	At 3/4T	At 1/4T	At 3/4T	At 1/4T	At 3/4T
ZV4281	SA508, Cl 2	Nozzle belt	--	--	--	+10	0.15	0.009	1.8E18	4.3E17	49	24	59	34
C-5062-1	SA533, B1	Upper shell	--	--	--	+4	0.12	0.013	2.4E18	5.7E17	52	25	56	29
C-5062-2	SA533, B1	Upper shell	--	--	--	-10	0.12	0.013	2.4E18	5.7E17	52	25	42	15
C-5070-1	SA533, B1	Lower shell	--	--	--	0	0.10	0.010	2.4E18	5.7E17	30	14	30	14
C-5070-2	SA533, B1	Lower shell	--	--	--	-10	0.10	0.010	2.4E18	5.7E17	35	17	25	7
WF-233	Weld	Upper circum. seam (100%)	+123	--	Yes	(+20)	(-)	(-)	1.8E18	4.3E17	134	66	154	86
WF-154	Weld	Middle circum. seam (100%)	-63	--	Yes	(+20)	(-)	(-)	2.4E18	5.7E17	145	71	165	91
WF-233	Weld	Lower circum. seam (100%)	-249	--	Yes	(+20)	(-)	(-)	1.3E16	3.2E15	12	Neg.	32	20
WF-29	Weld	Upper long. both (100%)	--	4/3	Yes	(+20)	(-)	(-)	2.1E18	5.1E17	103	51	123	71
WF-29	Weld	Lower long. (100%)	--	14	Yes	(+20)	(-)	(-)	2.4E18	5.7E17	111	54	131	74
WF-70	Weld	Lower long. (ID 73%)	--	14	Yes	(+20)	(-)	(-)	2.4E18	--	176	--	196	--
WF-29	Weld	Lower long. (OD 27%)	--	14	No	(+20)	(-)	(-)	--	5.7E17	--	54	--	74

(a) Per Regulatory Guide 1.99, Revision 1.

Notes: ( ): per BAW-10046P, March 1976.[3]
(-): per BAW-1511P, October 1980.[4]

Figure 8-1. Predicted Fast Neutron Fluence at Various Locations Through Reactor Vessel Wall for First 10 EFPY (Rancho Seco)

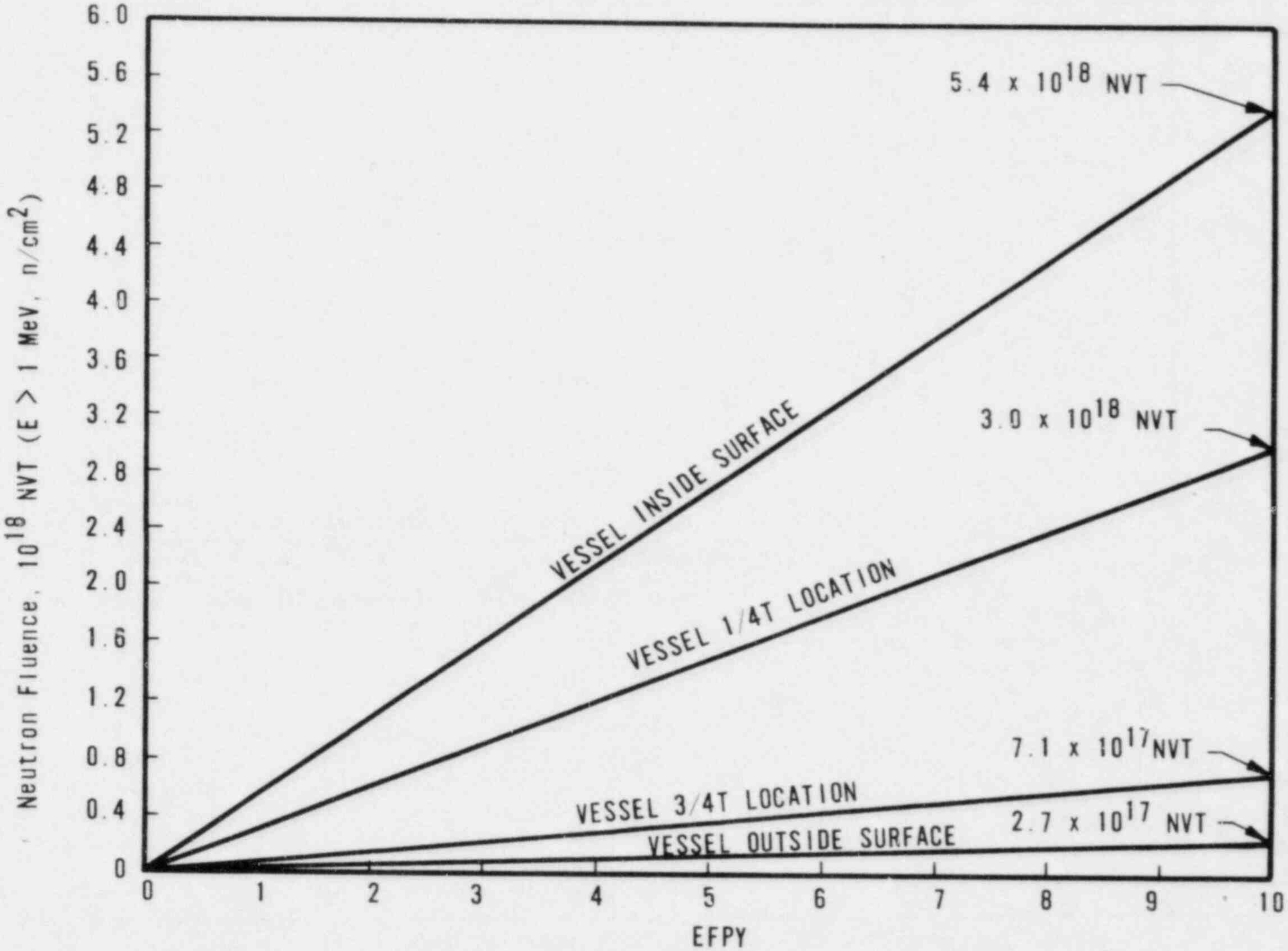

Figure 8-2. Reactor Vessel Pressure-Temperature Limit Curves for Normal Operation — Heatup, Applicable for First 8 EFPY

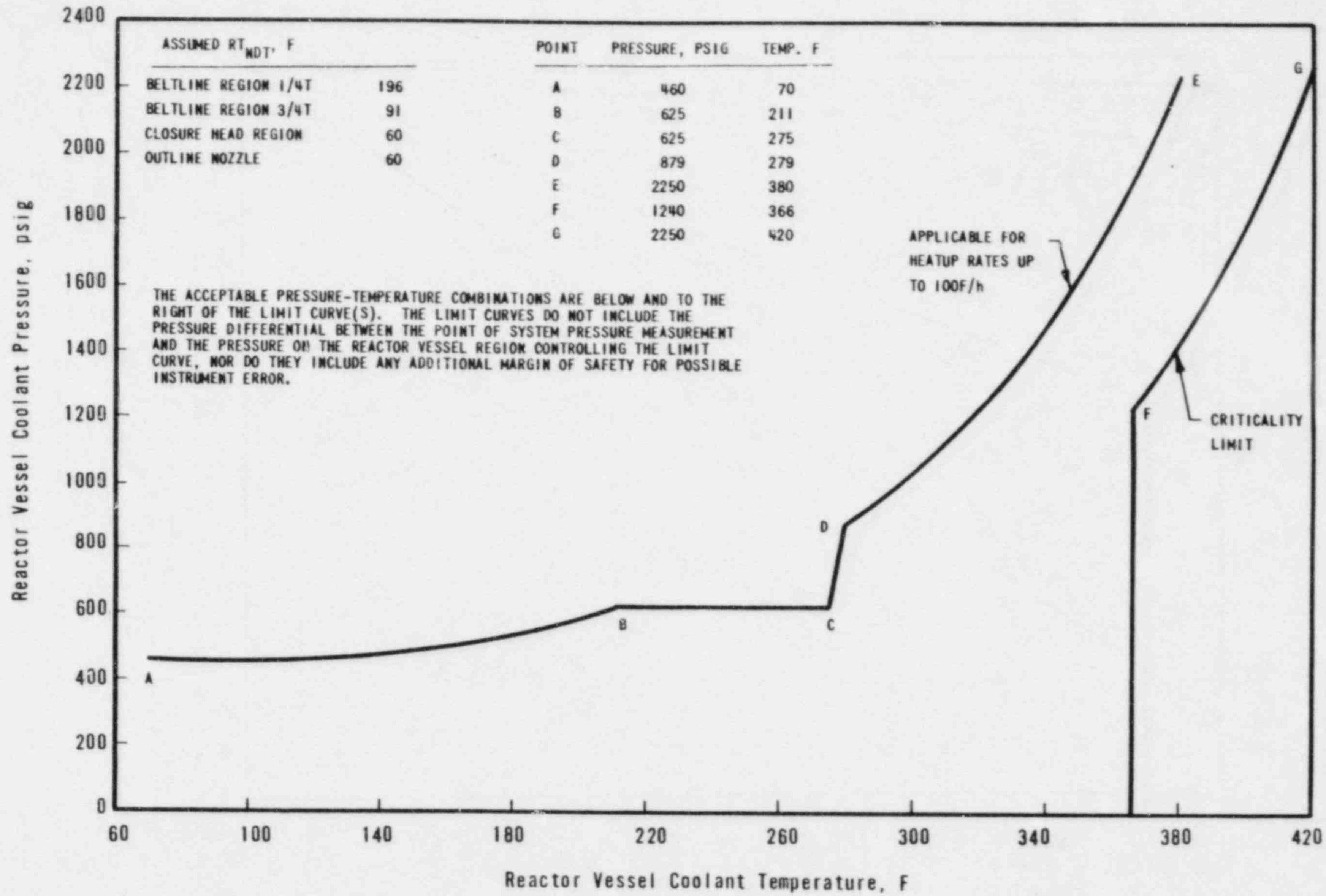

Figure 8-3. Reactor Vessel Pressure-Temperature Limit Curve for Normal Operation — Cooldown, Applicable for First 8 EFPY

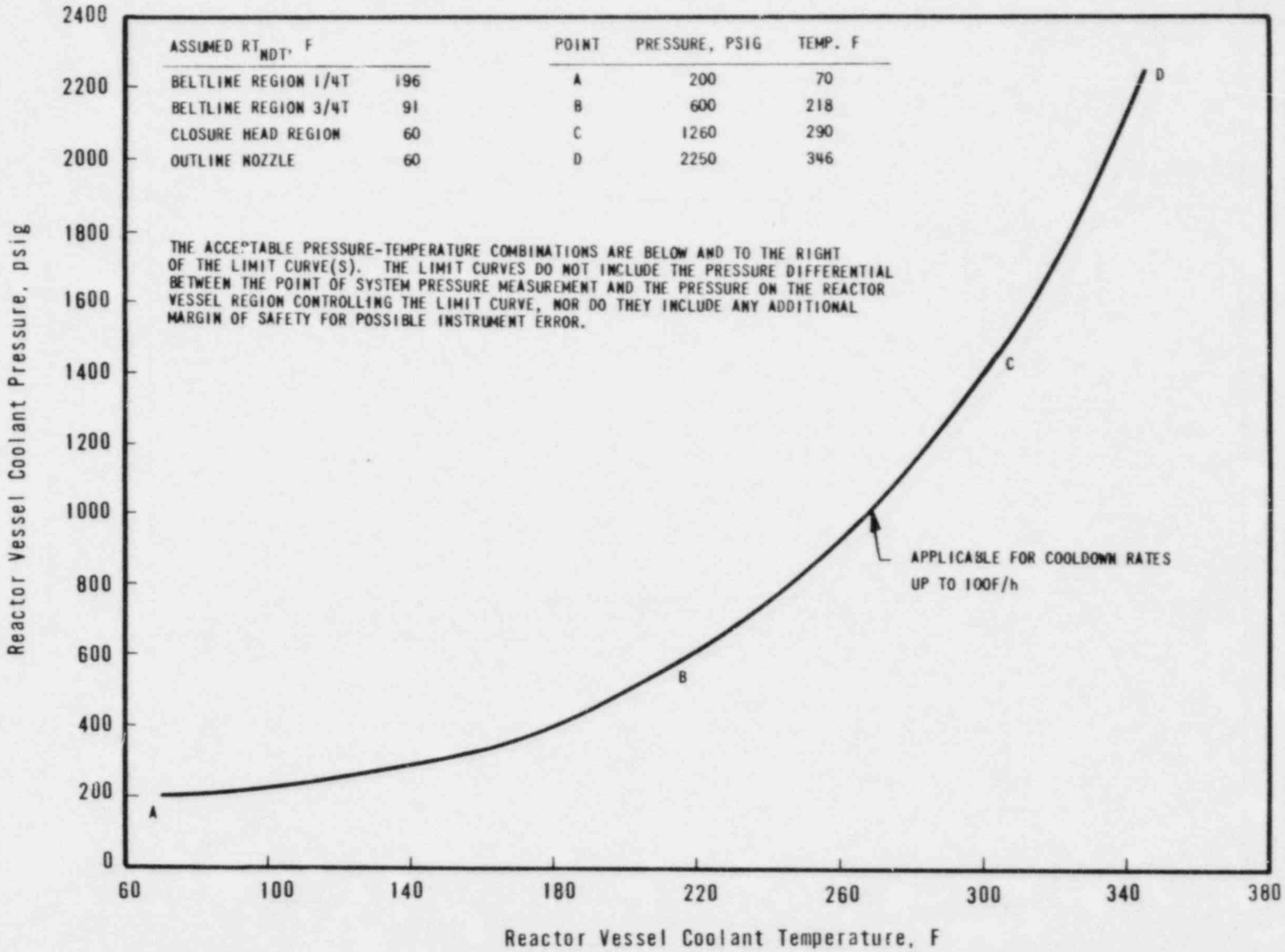

Figure 8-4. Reactor Vessel Pressure-Temperature Limit Curve for Inservice Leak and Hydrostatic Tests, Applicable for First 8 EFPY

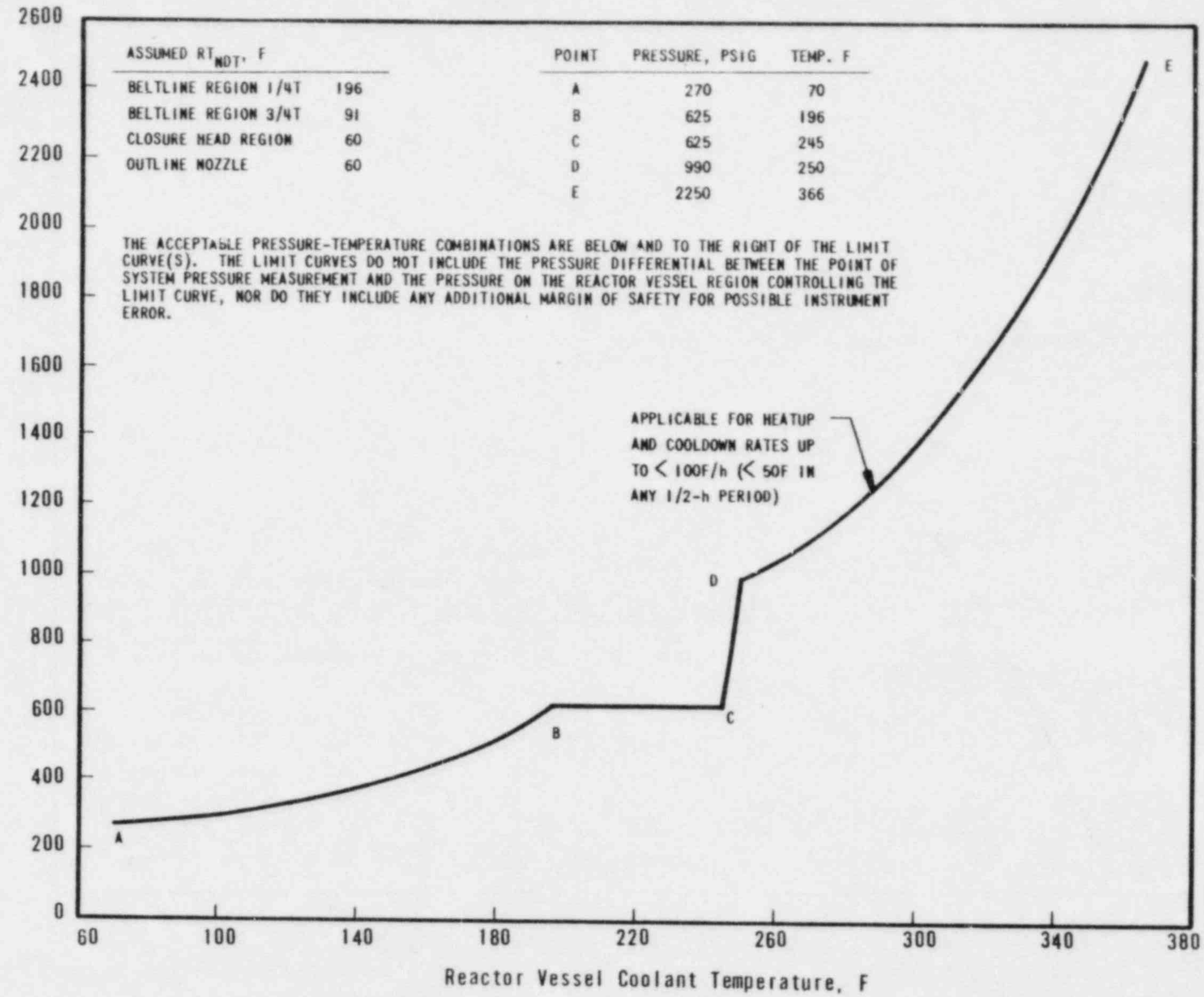

9. SUMMARY OF RESULTS

The analysis of the reactor vessel material contained in the first surveillance capsule RS1-B removed from the Rancho Seco Unit 1 pressure vessel led to the following conclusions:

1. The capsule received an average fast fluence of 3.99×10^{18} n/cm^2 (E > 1 Mev). The predicted fast fluence for the reactor vessel T/4 location at the end of the third fuel cycle is 9.6×10^{17} n/cm^2 (E > 1 Mev).

2. The fast fluence of 3.99×10^{18} n/cm^2 (E > 1 Mev) increased the RT_{NDT} of the capsule reactor vessel core region shell materials a maximum of 192F.

3. Based on the calculated fast flux at the vessel wall, an 80% load factor and the planned fuel management, the projected fast fluence that the Rancho Seco Unit 1 reactor pressure vessel will receive in 40 calendar years' operation is 1.62×10^{19} n/cm^2 (E > 1 Mev).

4. The increase in the RT_{NDT} for the base plate material was not in good agreement with that predicted by the currently used design curves of ΔRT_{NDT} versus fluence, but the prediction techniques are conservative.

5. The increase in the RT_{NDT} for the weld metal was not in good agreement with that predicted by the currently used design curves of ΔRT_{NDT} versus fluence because of possible uncertainties in chemical composition.

6. The current techniques used for predicting the change in Charpy impact upper shelf properties due to irradiation are conservative.

7. The analysis of the neutron dosimeters demonstrated that the analytical techniques used to predict the neutron flux and fluence were accurate.

8. The thermal monitors indicated that the capsule design was satisfactory for maintaining the specimens within the desired temperature range.

10. SURVEILLANCE CAPSULE REMOVAL SCHEDULE

Based on the post-irradiation test results of capsule RS1-B the following schedule is recommended for examination of the remaining capsules in the Rancho Seco Unit 1 reactor vessel surveillance program:

	Evaluation schedule[a]			
		Est vessel fluence, 10^{19} n/cm^2		
Capsule ID	Est capsule fluence 10^{19} n/cm^2	Surface	1/4T	Est date data available[b]
RS1-D[c]	0.7	0.29	0.17	1982
RS1-A	1.8	0.57	0.33	1987
RS1-F[c]	3.2	0.69	0.40	1989
RS1-E	3.2	0.75	0.43	1990
RS1-C	4.2	0.86	0.50	1992

[a] In accordance with BAW-10100A and E-185-79 as modified by BAW-1543.

[b] Estimated date based on 0.8 plant operation factor.

[c] Capsules contain weld metal compact fracture specimens.

11. CERTIFICATION

The specimens were tested, and the data obtained from Rancho Seco Unit 1 surveillance capsule RS1-B were evaluated using accepted techniques and established standard methods and procedures in accordance with the requirements of 10 CFR 50, Appendixes G and H.

PE. 24Feb1982

A. L. Lowe, Jr., P.E. Date
Project Technical Manager

This report has been reviewed for technical content and accuracy.

J. D. Aadland 2/24/82

J. D. Aadland Date
Component Engineering

APPENDIX A

Reactor Vessel Surveillance Program —
Background Data and Information

1. Material Selection Data

The data used to select the materials for the specimens in the surveillance program, in accordance with E-185-73, are shown in Table A-1. The locations of these materials within the reactor vessel are shown in Figures A-1 and A-2.

2. Definition of Beltline Region

The beltline region of Rancho Seco Unit 1 was defined in accordance with the data given in BAW-10100A.

3. Capsule Identification

The capsules used in the Rancho Seco Unit 1 surveillance program are identified below by identification number, type, and location.

Capsule Cross Reference Data

Number	Type
RS1-A	III
RS1-B	IV
RS1-C	III
RS1-D	IV
RS1-E	III
RS1-F	IV

4. Specimens per Surveillance Capsule

See Tables A-2, A-3 and A-4.

Table A-1. Unirradiated Impact Properties and Residual Element Content Data of Beltline Region Materials Used for Selection of Surveillance Program Materials — Rancho Seco Unit 1

Material ident, heat No.	Material type	Beltline region location	Distance, core midplane to weld centerline, cm	Drop wt, T_{NDT}, F	Charpy data, CVN: Longitudinal At 10F ft-lb	Transverse: 50 ft-lb, F	35 MLE, F	USE, ft-lb	RT_{NDT}, F	Chemistry, %: Cu	P	S	Ni
ZV4281	SA-508, Cl 2	Nozzle belt	--	10		--	--	131	10	0.15	0.009	0.005	--
C-5062-1	SA-533, Gr B	Upper shell	--	-10	50 (10 Cvs)	80	--	90	4	0.12	0.013	0.017	0.60
C-5062-2	SA-533, Gr B	Upper shell	--	-10	60 (10 Cvs)	80	--	88	-10	0.12	0.013	0.017	0.60
C-5070-1	SA-533, Gr B	Lower shell	--	-20	46,56,61	--	--	92	0	0.10	0.010	0.015	0.58
C-5070-2	SA-533, Gr B	Lower shell	--	-20	75,60,63	100	--	90	-10	0.10	0.010	0.015	0.58
WF-29	Weld	Upper long. seam (100%)	--	--	49,39,45	--	--	--	--	0.16	0.017	0.010	0.29
WF-233	Weld	Upper circ seam (100%) OD	123	--	43,30,26	--	--	--	--	0.22	0.015	0.016	0.55
WF-154	Weld	Middle circ seam (100%)	-62	--	41,37,43	--	--	--	--	0.20	0.015	0.021	0.59
WF-29	Weld	Lower long. seam (27%)	--	--	49,39,45	--	--	--	--	0.16	0.017	0.010	0.29
WF-70	Weld	Lower long. seam (73%)	--	--	39,35,44	--	--	--	--	0.27	0.014	0.011	0.46
WF-233	Weld	Lower circ seam (100%)	-249	--	43,30,26	--	--	--	--	0.22	0.015	0.016	0.55

Table A-2. Test Specimens for Determining Material Baseline Properties

Material description	No. of test specimens			
	Tension			
	70F	600F[a]	CVN impact	Compact-fracture[b]
Heat LL				
Base metal				
Transverse direction	3	3	15	--
Longitudinal direction	3	3	15	--
Heat-affected zone (HAZ)				
Transverse direction	3	3	15	--
Longitudinal direction	3	3	15	--
Total	12	12	60	--
Heat MM				
Base metal				
Transverse direction	3	3	15	--
Longitudinal direction	3	3	15	--
Heat-affected zone (HAZ)				
Transverse direction	3	3	15	--
Longitudinal direction	3	3	15	--
Total	12	12	60	--
Weld metal				
Longitudinal direction	3	3	15	8 1/2 TCT 4 1 TCT

[a]Test temperature to be the same as irradiation temperature.

[b]Test temperature to be determined from shift in impact transition curves after irradiation exposure.

Table A-3. Specimens in Upper Surveillance Capsules (Designation A, C, and E)

Material description	No. of test specimens: Tension	CVN impact
Weld metal	2	12
Weld, HAZ		
Heat LL, transverse	--	12
Heat MM, transverse	--	6
Base metal		
Heat LL, transverse	2	12
Heat MM, transverse	--	6
Correlation material	--	6
Total per capsule	4	54

Table A-4. Specimens in Lower Surveillance Capsules (Designation B, D, and F)

Material description	No. of test specimens: Tension	CVN impact	1/2 T compact fracture[(a)]
Weld metal	2	12	8
Weld, HAZ			
Heat LL, transverse	--	12	--
Base metal			
Heat LL, transverse	2	12	--
Total per capsule	4	36	8

[(a)] Compact fracture specimens precracked per ASTM E399-72.

Figure A-1. Location and Identification of Materials Used in Fabrication of Rancho Seco Unit 1 Reactor Pressure Vessel

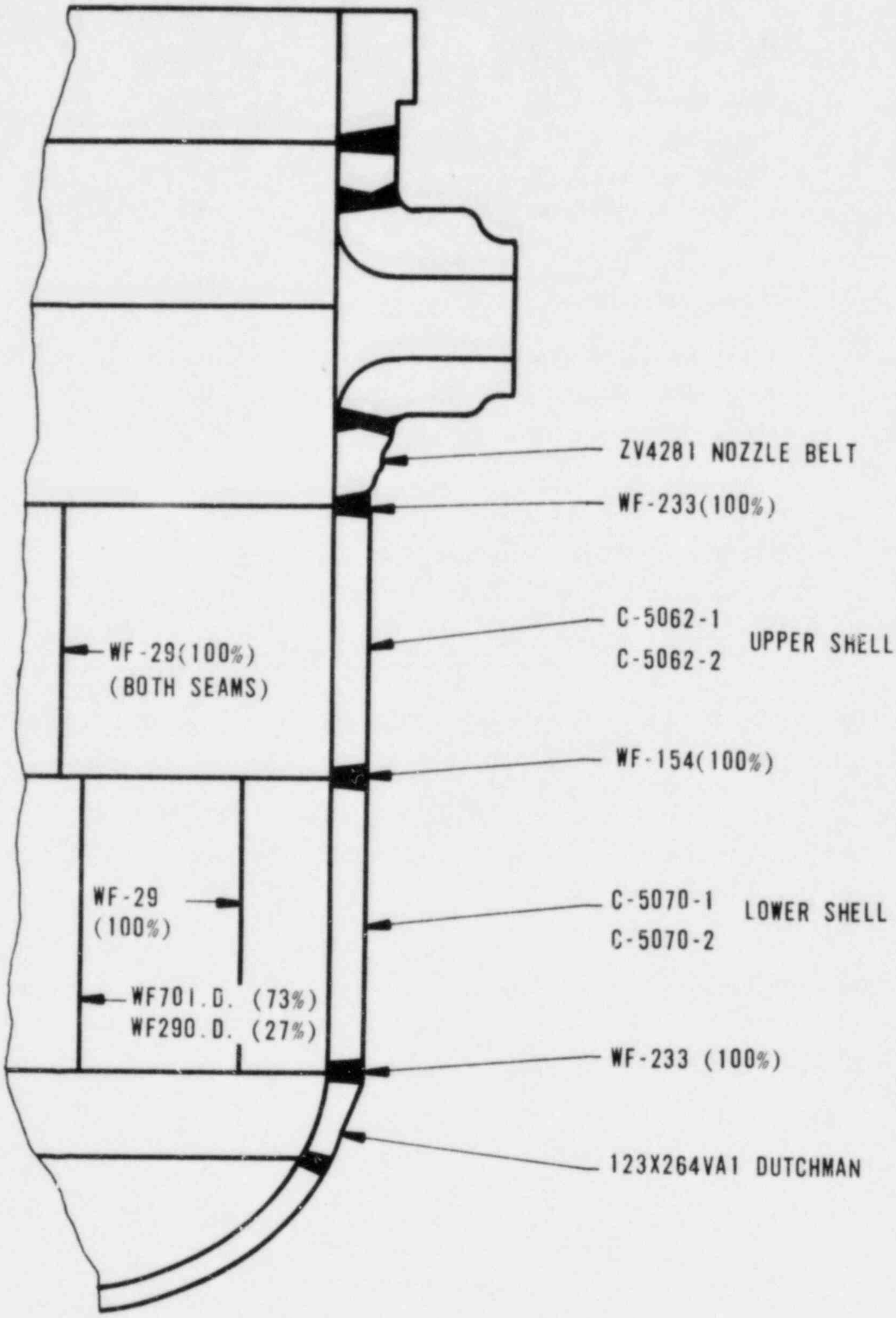

Figure A-2. Location of Longitudinal Welds in Upper and Lower Shell Courses

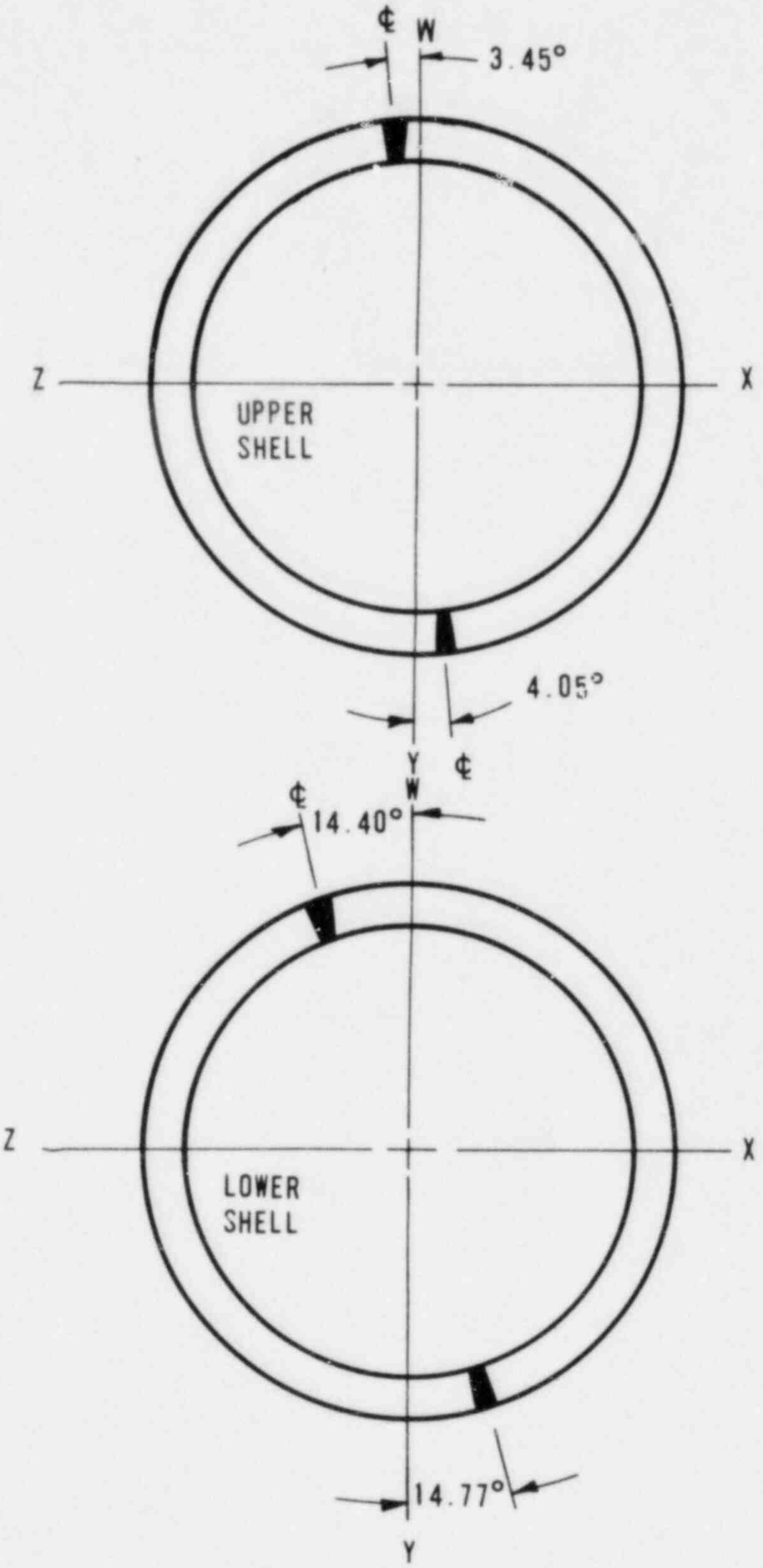

APPENDIX B

Preirradiation Tensile Data

Table B-1. Preirradiation Tensile Properties of Shell Plate Material, Heat C-5062-1

Specimen No.	Test temp, F	Strength, psi		Elongation, %		Red'n of area, %
		Yield	Ultimate	Uniform	Total	
Base Metal, Transverse						
LL-606	73	62.8	83.4	16.2	26.9	64.4
LL-607	73	64.1	83.8	16.7	27.1	67.3
LL-619	73	64.7	84.1	16.4	27.9	66.4
Mean	73	63.9	83.8	16.4	27.3	66.0
Std dev'n	73	0.97	0.35	0.25	0.53	1.48
LL-621	580	57.5	83.4	18.2	26.4	53.6
LL-622	581	58.1	82.5	15.9	19.9	60.2
LL-623	582	56.9	82.8	19.2	26.1	57.7
Mean	580	57.5	82.9	17.8	24.1	57.2
Std dev'n	580	0.60	0.46	1.69	3.67	3.33
Heat-Affected Zone Transverse						
LL-301	73	62.5	83.8	9.9	21.5	64.4
LL-302	73	60.6	81.9	9.7	20.5	66.0
LL-303	73	65.0	84.7	10.5	19.0	63.0
Mean	73	62.7	83.5	10.0	20.3	64.5
Std dev'n	73	2.21	1.43	0.42	1.26	1.50
LL-304	580	68.8	81.6	8.1	16.6	58.5
LL-305	582	64.1	81.3	9.4	16.4	59.2
LL-306	580	61.9	82.5	10.0	17.9	57.7
Mean	580	64.9	81.8	9.2	17.0	58.5
Std dev'n	580	3.52	0.62	0.97	0.81	0.75

Table B-2. Preirradiation Tensile Properties of Weld Metal, WF-193

Specimen No.	Test temp, F	Strength, psi		Elongation, %		Red'n of area, %
		Yield	Ultimate	Uniform	Total	
MM-002	73	67.5	83.1	16.2	30.4	63.7
MM-014	73	67.5	83.8	16.2	27.5	62.3
Mean	73	67.5	83.5	16.2	29.0	63.0
Std dev'n	73	0	0.49	0	2.05	0.99
MM-015	581	61.3	81.9	14.9	21.0	51.7
MM-017	576	61.6	80.0	13.6	21.6	55.9
MM-018	581	61.9	80.0	12.5	18.9	49.3
Mean	580	61.6	80.6	13.7	20.5	52.3
Std dev'n	580	0.30	1.10	1.20	1.42	3.34

APPENDIX C

Preirradiation Charpy Impact Data

Table C-1. Preirradiation Charpy Impact Data for Base Material, Transverse Direction, Heat C-5062-1

Specimen No.	Test temp, F	Absorbed energy, ft-lb	Lateral expansion, 10^{-3} in.	Shear fracture, %
LL-637	-79	5.5	4	0
LL-669	-40	14.0	13	0
LL-625	-2	30.5	30	5
LL-650	0	30.0	29	5
LL-653	0	25.5	26	5
LL-654	+39	45.0	40	15
LL-672	+70	66.0	56	25
LL-689	+70	56.0	54	20
LL-681	+74	65.0	60	60
LL-661	+130	93.0	72	100
LL-645	+218	81.0	73	100
LL-699	+582	94.0	78	100

Table C-2. Preirradiation Charpy Impact Data for Base Material, HAZ, Transverse Direction, Heat C-5062-1

Specimen No.	Test temp, F	Absorbed energy ft-lb	Lateral expansion, 10^{-3} in.	Shear fracture %
LL-318	-80	20.0	17	5
LL-306	-79	21.5	21	15
LL-351	-59	43.0	25	15
LL-359	-40	61.0	50	70
LL-332	-2	67.5	53	100
LL-322	0	60.0	49	70
LL-349	0	64.5	48	45
LL-376	+40	93.0	72	100
LL-385	+74	97.0	71	100
LL-360	+130	89.5	70	100
LL-327	+213	83.0	75	100
LL-379	+280	101.5	77	100
LL-370	+338	122.5	83	100
LL-380	+590	132.0	81	100

Table C-3. Preirradiation Charpy Impact Data for Weld Metal, WF-193

Specimen No.	Test temp, F	Absorbed energy, ft-lb	Lateral expansion, 10^{-3} in.	Shear fracture, %
MM-066	-79	21.5	21	10
MM-062	-40	25.0	28	20
MM-064	-40	15.0	14	0
MM-073	-2	39.0	42	30
MM-071	0	34.5	34	20
MM-074	0	35.0	39	50
MM-051	+40	51.0	53	80
MM-083	+70	56.0	59	90
MM-086	+70	56.0	57	95
MM-087	+74	66.0	66	100
MM-081	+129	66.0	69	100
MM-019	+218	68.5	69	100
MM-059	+338	74.5	79	100
MM-025	+590	67.5	79	100

Figure C-1. Charpy Impact Data From Unirradiated Base Metal, Transverse Orientation

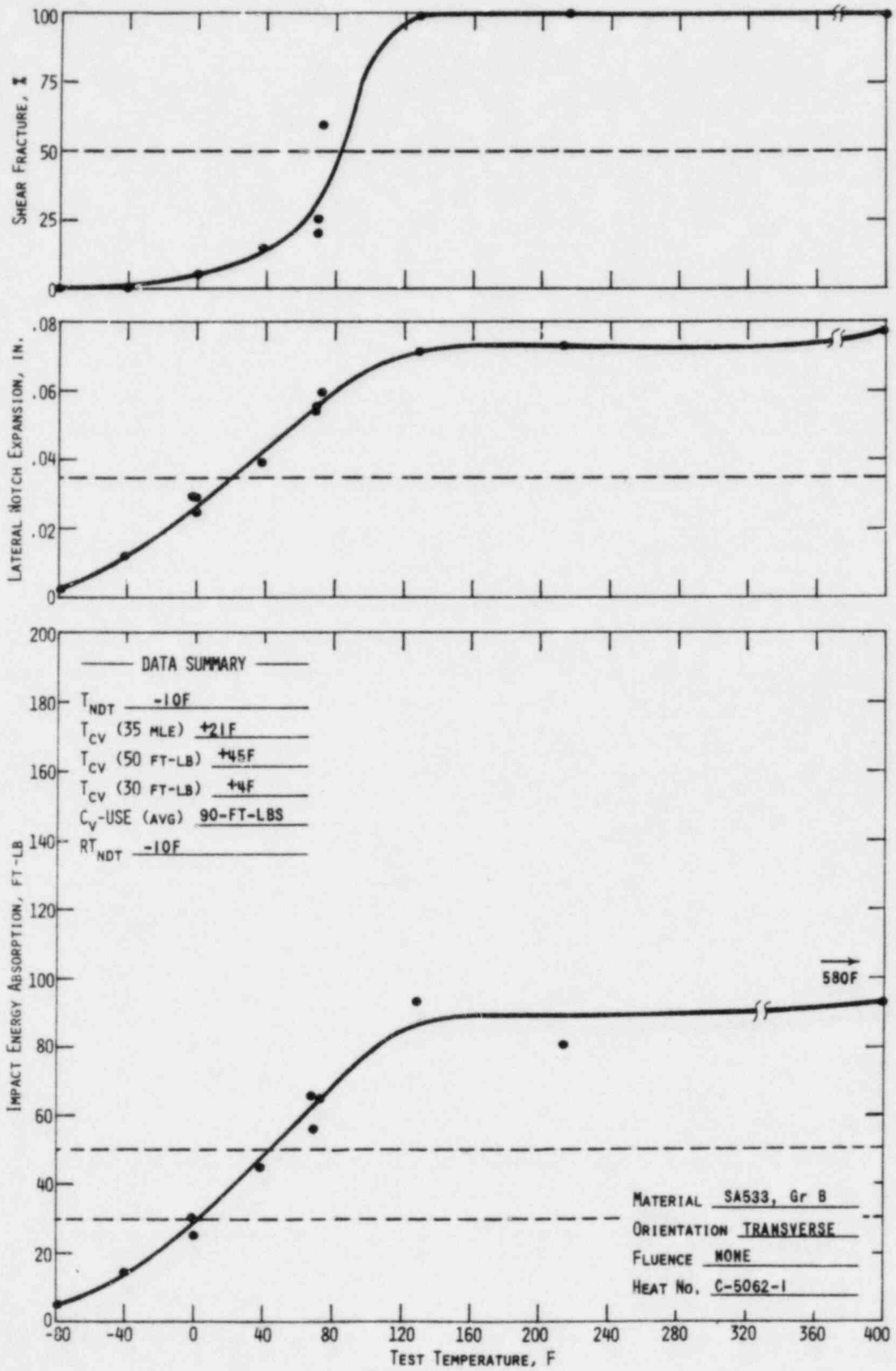

Figure C-2. Charpy Impact Data From Unirradiated Base Metal, Heat-Affected Zone, Transverse Orientation

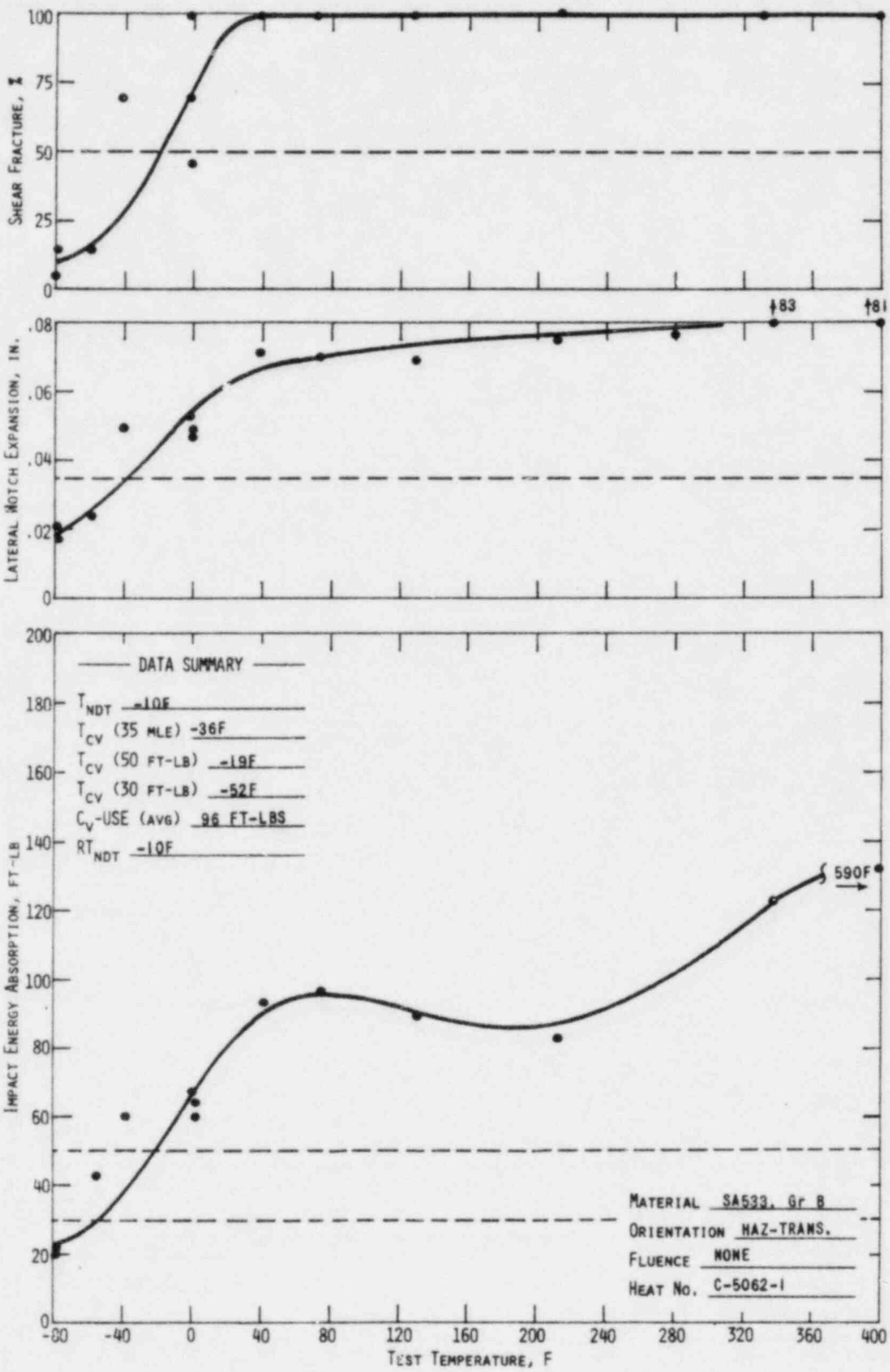

Figure C-3. Charpy Impact Data From Unirradiated Weld Metal

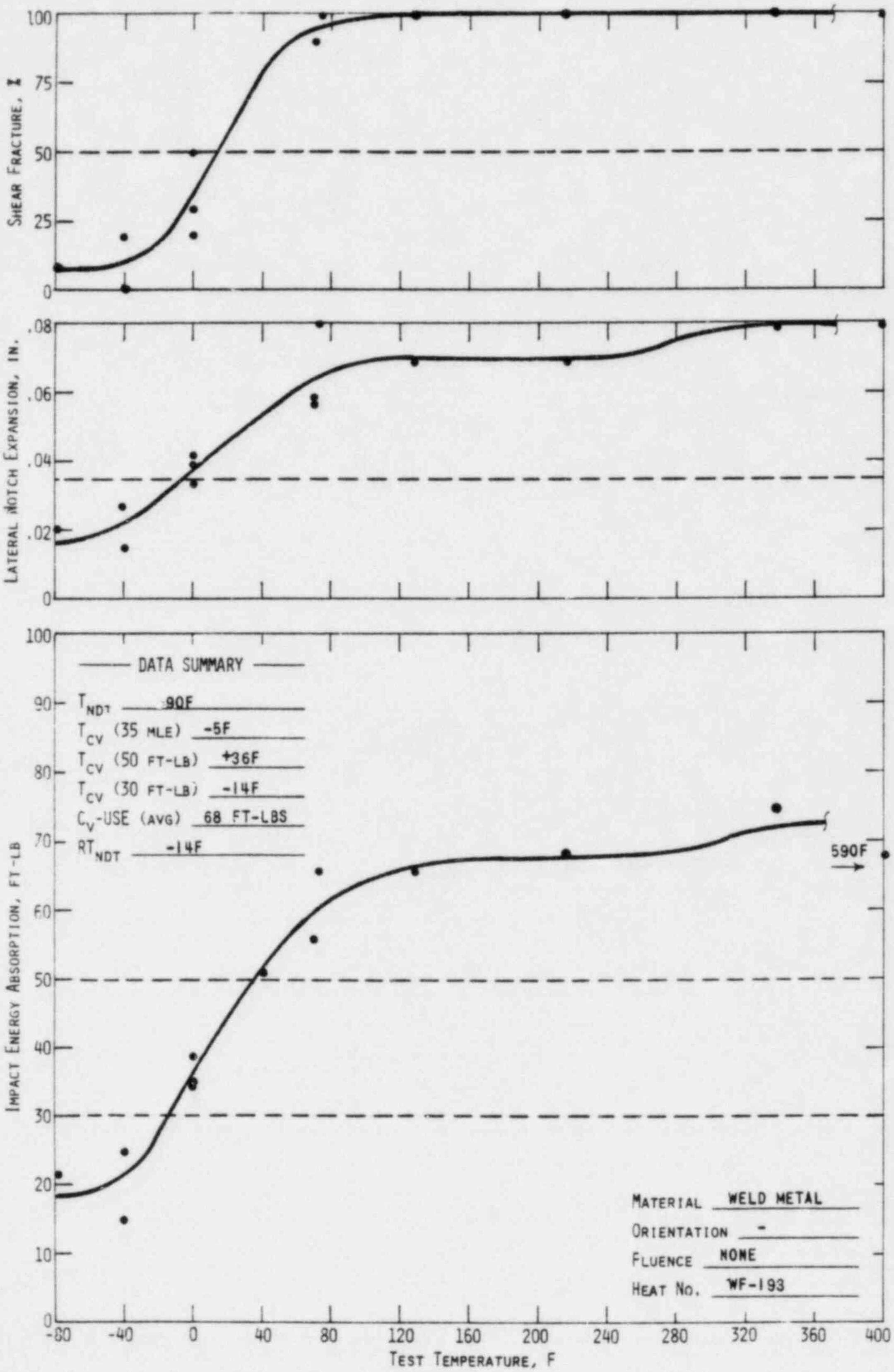

APPENDIX D

Fluence Analysis Procedures

Analytical Method

Energy-dependent neutron fluxes at the detector locations were determined by a discrete ordinates solution of the Boltzmann transport equation with the two-dimensional code DOT3.5.[5] The Rancho Seco Unit 1 reactor was modeled from the core out to the primary concrete shield in R-theta geometry [based on a plan view along the core midplane and one-eighth core symmetry in the azimuthal (theta) dimension]. Also included was an explicit model of a surveillance capsule assembly in the downcomer region. The reactor model contained the following regions: core, liner, bypass coolant, core barrel, inlet coolant, thermal shield, inlet coolant (downcomer), pressure vessel, cavity, and concrete shield. Input data to the code included a PDQ calculated pin-by-pin, time-averaged power distribution, CASK23E 22-group microscopic neutron cross sections[6], S_8 order of angular quadrature, and P_3 expansion of the scattering cross section matrix. Reactor conditions — power distribution, temperature, and pressure — were averaged over the irradiation period. A more detailed description of the calculational procedure (except for capsule modeling) is presented in reference 7.

Because of computer storage limitations, it was necessary to use two geometric models to cover the distance from core to primary shield. A boundary source output from model A (core to downcomer region) was used as input to model B (thermal shield to primary shield), which included the capsule assembly. This procedure was repeated with a Davis-Besse, cycle 1, calculational model to account for the second period of capsule irradiation. In those cases where the capsule "shadowed" the maximum flux location in the pressure vessel, a model C (model B without a capsule assembly) was used to obtain vessel flux unperturbed by the presence of a capsule. For a reactor without surveillance capsules, an additional model A and model C were calculated. In this way the effect of the specific power distribution in Rancho Seco for cycles 1 through 3 on vessel fluence was included in the calculation.

Flux output from the DOT3.5 calculations required only an axial distribution correction to provide absolute values. An axial shape factor (local:average axial flux ratio) was obtained from predicted fuel burnup distributions in those peripheral fuel assemblies nearest the capsule location. This procedure assumes that axial fast flux shape in the capsule and the pressure vessel is the same as axial power distribution in the closest fuel assembly. In the 177-FA reactor geometry this is considered to be a conservative assumption be-

because axial shape should tend to flatten as distance from the core increases. Based on an average over an elevation corresponding to the capsule length, a factor of 1.26 was applied to capsule data in Rancho Seco and 1.17 to capsule data in Davis Besse; and a maximum value of 1.17 was applied to the pressure vessel in Rancho Seco. Axial factors for the capsules were time-averaged over their respective irradiation periods, and for the pressure vessel was time-averaged over the first 3 cycles.

The calculation described above provides the neutron flux as a function of energy at the capsule position. These calculated data are used in the following equations to obtain the activities used for comparison with the experimental values. The equation for the calculated activity D (in μCi/g) is as follows:

$$D_i = \frac{N}{A_n} \frac{1}{3.7 \times 10^4} f_i \sum_E \sigma_n(E)\phi(e) \sum_{j=1}^{M} F_j(1 - e^{-\lambda_i t_j})e^{-\lambda_i(T-\tau_j)} \qquad \text{(D-1)}$$

where

N = Avogadro's number,

A_n = atomic weight of target material n,

f_i = either weight fraction of target isotope in nth material or fission yield of desired isotope,

$\sigma_n(E)$ = group-averaged cross sections for material n (listed in Table E-3),

$\phi(E)$ = group-averaged fluxes calculated by DOT3.5 analysis,

F_j = fraction of full power during jth time interval, t_j,

λ_i = decay constant of the ith isotope,

T = sum of total irradiation time, i.e., residual time in reactor, and wait time between reactor shutdown and counting,

t_j = interval of power history,

τ_j = cumulative time from reactor start-up to end of jth time period, i.e.,

$$\tau_j = \sum_{k=1}^{j} t_k.$$

The normalizing constant C is obtained from the ratio of measured to calculated activities.

$$C = \frac{D_i(\text{measured})}{D_i(\text{calculated})}. \tag{D-2}$$

With C specified, the neutron fluence greater than 1 Mev can be calculated from

$$\phi(E > 1.0\ \text{Mev}) = C \sum_{E=1}^{15\ \text{Mev}} \phi(E) \sum_{j=1}^{M} F_j t_j \tag{D-3}$$

where M is the number of irradiation time intervals; the other values are defined above. The normalization constant for the RS1-B capsule was determined to be 1.03 (Table D-1). Although this normalization is strictly correct only at the capsule location, it was considered applicable to all locations in the reactor model. (B&W 177-FA reactors have essentially the same configurations and materials.) In the calculational model, pressure vessel and capsule are separated by only 15 cm of water, and it is very unlikely that any significant change in accuracy would occur over that distance.

Vessel Fluence Extrapolation

For up-to-date operation, fluence values in the pressure vessel are calculated as described above. Extrapolation of future operation is required for prediction of vessel life based on minimum upper shelf energy and for calculation of pressure-temperature operation curves. Three time periods are considered: (1) to-date operation for which vessel fluence has been calculated, (2) designed future fuel cycles for which PDQ calculations have been performed for fuel management analysis of reload cores, and (3) future fuel cycles for which no analyses exist. Data from time period 1 are extrapolated through time period 2 based on the premise that ex-core flux is proportional to fast flux that escapes the core boundary. Thus, for the vessel,

$$\phi_{v,C} = \frac{\phi_{e,C}}{\phi_{e,R}} \times \phi_{v,R}$$

where the subscripts are defined as v = vessel, e = core escape, R = reference cycle, and C = a future fuel cycle. Core escape flux is available from PDQ output. Extrapolation from time period 2 through time period 3 is based on the last fuel cycle in 2 having the same relative power distribution as an "equilibrium" fuel cycle. Generally, the designed fuel cycles include several cycles into the future. Therefore, the last cycle in time period 2 should be representative of an "equilibrium" cycle. Data for RS1-B are listed in Table D-2.

This procedure is considered preferable to the alternative of assuming that lifetime fluence is based on a single, hypothetical "equilibrium" fuel cycle because it accounts for all known power distributions. In addition, it reduces errors that may result from the selection of a hypothetical "equilibrium" cycle.

Table D-1. Capsule Normalization Constant

	A measured activity,[a] μCi/g	B calculated activity, μCi/g	C = A/B normalization constant [b]
$^{54}Fe(n,p)^{54}Mn$	9.84(+2)	1.22(+3)	0.81
$^{58}Ni(n,p)^{58}Co$	1.76(+3)	2.11(+3)	0.83
$^{238}U(n,f)^{137}Cs$	4.88	4.75	1.03
$^{237}Np(n,f)^{137}Cs$	3.01(+1)	2.91(+1)	1.03

(a) Average of four dosimeter wires from Table E-2 referenced to a capsule average position.

(b) Average of ^{137}Cs reactions (1.03) was selected as the normalization constant.

Table D-2. Extrapolation of Pressure Vessel Fluence

Cycle	Core escape flux, n/cm²-s	Time, EFPY	Cumul. time, EFPY	Vessel flux, n/cm²-s	Vessel fluence, n/cm² Time interval	Vessel fluence, n/cm² Cumulative
1+2+3	0.62(+14)	2.82	2.82	1.94(+10)	1.73(+18)	1.73(+18)
4	0.546(+14)	0.94	3.76	1.71(+10)[a]	5.08(+17)	2.24(+18)
5	0.503(+14)	1.00	4.76	1.57(+10)[a]	4.95(+17)	2.74(+18)
>5[b]	0.503(+14)	3.24	8.0	1.57(+10)[a]	1.61(+18)	4.35(+18)
>5[b]	0.503(+14)	24.0	32.0	1.57(+10)[a]	1.19(+19)	1.62(+19)

[a] Predicted value based on proportionality of core escape flux.

[b] Cycle 5 assumed to be equilibrium cycle for future operation.

APPENDIX E

Capsule Dosimetry Data

Table E-1 lists the composition of the threshold detectors and the equivalent cadmium thickness used to reduce competing thermal reactions. Table E-2 shows capsule RS1-B measured activity per gram of target material (i.e., per gram of uranium, nickel, etc.). Activation cross sections for the various materials were flux-weighted with a ^{235}U fission spectrum (Table E-3).

Table E-1. Detector Composition and Shielding

Monitors	Shielding	Reaction
10.38% U-Al	Cd-Ag 0.02676 in. Cd	$^{238}U(n,f)$
1.44% Np-Al	Cd-Ag 0.02676 in. Cd	$^{237}Np(n,f)$
Ni 100%	Cd-Ag 0.02676 in. Cd	$^{58}Ni(n,p)^{58}Co$
0.56 wt % Co-Al	Cd-0.040 in. Cd	$^{59}Co(n,\gamma)^{60}Co$
0.56 wt % Co-Al	None	$^{59}Co(n,\gamma)^{60}Co$
Fe 100%	None	$^{54}Fe(n,p)^{54}Mn$

Table E-2. Capsule RS1-B Dosimeter Activation Measurements

Dosimeter material	Post-irr weight, g	Reaction	Radio-nuclide	Nuclide activity, μCi	Specific activity, μCi/g	Activity, μCi/g of target
Dosimeter BD-5						
Co-Al(bare)	0.0163	$^{59}Co(n,\gamma)$	^{60}Co	24.26	1490	266000
Co-Al(Cd)	0.0200	$^{59}Co(n,\gamma)$	^{60}Co	28.45	1420	254000
Ni	0.1353	$^{58}Ni(n,p)$	^{58}Co	183.6	1360	2000
		$^{60}Ni(n,p)$	^{60}Co	0.4935	3.65	13.9
Fe	0.1585	$^{54}Fe(n,p)$	^{54}Mn	9.982	63.0	1080
		$^{58}Fe(n,\gamma)$	^{59}Fe	24.32	153	46500
^{238}U-Al	0.0491	$^{238}U(n,F)$	^{95}Zr	0.4757	9.69	94.1
			^{103}Ru			
			^{106}Ru	0.148	3.01	29.3
			^{137}Cs	0.02586	0.527	5.11
			^{144}Ce	0.2084	6.28	61.0
^{237}Np-Al	0.0723	$^{237}Np(n,F)$	^{95}Zr	0.6712	9.28	645
			^{103}Ru			
			^{106}Ru	0.161	2.23	155
			^{137}Cs	0.03436	0.475	33.0
			^{144}Ce	0.3616	5.00	347
Dosimeter BD-6						
Co-Al(bare)	0.0171	$^{59}Co(n,\gamma)$	^{60}Co	Defective Dosimeter Wire		
Co-Al(Cd)	0.0200	$^{59}Co(n,\gamma)$	^{60}Co	25.33	1270	227000
Ni	0.1346	$^{58}Ni(n,p)$	^{58}Co	155.1	1150	1700
		$^{60}Ni(n,p)$	^{60}Co	0.4395	3.26	12.5
Fe	0.1515	$^{54}Fe(n,p)$	^{54}Mn	8.408	55.5	954
		$^{58}Fe(n,\gamma)$	^{59}Fe	20.13	133	40300

Table E-2. (Cont'd)

Dosimeter material	Post-irr weight, g	Reaction	Radio-nuclide	Nuclide activity, μCi/g	Specific activity, μCi/g	Activity, μCi/g of target
^{238}U-Al	0.0457	^{238}U(n,F)	^{95}Zr	0.3683	8.06	78.2
			^{103}Ru			
			^{106}Ru	0.125	2.74	26.6
			^{137}Cs	0.02173	0.475	4.62
			^{144}Ce	0.2574	5.63	54.7
^{237}Np-Al	0.0392	^{237}Np(n,F)	^{95}Zr	0.2985	7.62	529
			^{103}Ru			
			^{106}Ru	0.0754	1.92	134
			^{137}Cs	0.01569	0.400	27.8
			^{144}Ce	0.1494	3.81	265
Dosimeter BD-7						
Co-Al(bare)	0.0165	$^{59}Co(n,\gamma)$	^{60}Co	29.71	1800	322000
Co-Al(Cd)	0.0194	$^{59}Co(n,\gamma)$	^{60}Co	34.45	1780	317000
Ni	0.1355	^{58}Ni(n,p)	^{58}Co	207.7	1530	2260
		^{60}Ni(n,p)	^{60}Co	0.5761	4.25	16.2
Fe	0.1525	^{54}Fe(n,p)	^{54}Mn	11.61	76.1	1310
		$^{58}Fe(n,\gamma)$	^{59}Fe	27.21	178	54100
^{238}U-Al	0.0632	^{238}U(n,F)	^{95}Zr	0.7873	12.5	121
			^{103}Ru			
			^{106}Ru	0.249	3.94	38.2
			^{137}Cs	0.04211	0.666	6.47
			^{144}Ce	0.5046	7.98	77.5
^{237}Np-Al	0.0467	^{237}Np(n,F)	^{95}Zr	0.5225	11.2	777
			^{103}Ru			
			^{106}Ru	0.117	[illegible].50	174
			^{137}Cs	0.02538	0.543	37.7
			^{144}Ce	0.2711	5.80	403

Table E-2. (Cont'd)

Dosimeter material	Post-irr weight, g	Reaction	Radio-nuclide	Nuclide activity, µCi	Specific activity, µCi/g	Activity, µCi/g of target
Dosimeter BD-8						
Co-Al(bare)	0.0157	$^{59}Co(n,\gamma)$	^{60}Co	27.00	1720	307000
Co-Al(Cd)	0.0202	$^{59}Co(n,\gamma)$	^{60}Co	33.48	1660	296000
Ni	0.1317	$^{58}Ni(n,p)$	^{58}Co	191.3	1450	2140
		$^{60}Ni(n,p)$	^{60}Co	0.5335	4.05	15.5
Fe	0.1541	$^{54}Fe(n,p)$	^{54}Mn	10.70	69.4	1190
		$^{58}Fe(n,\gamma)$	^{59}Fe	25.68	167	50500
^{238}U-Al	0.0665	$^{238}U(n,F)$	^{95}Zr	0.7862	11.8	115
			^{103}Ru			
			^{106}Ru	0.242	3.64	35.3
			^{137}Cs	0.04277	0.643	6.24
			^{144}Ce	0.5038	7.58	73.6
^{237}Np-Al	0.0408	$^{237}Np(n,F)$	^{95}Zr	0.4374	10.7	744
			^{103}Ru			
			^{106}Ru	0.109	2.67	186
			^{137}Cs	0.02346	0.0575	39.9
			^{144}Ce	0.2363	5.79	402

Table E-3. Dosimeter Activation Cross Sections[a]

G	Energy range, Mev	Cross sections, b/atom ^{237}Np	^{238}U	^{58}Ni	^{54}Fe
1	12.2 - 15	2.323	1.050	4.830(-1)	4.133(-1)
2	10.0 - 12.2	2.341	9.851(-1)	5.735(-1)	4.728(-1)
3	8.18 - 10.0	2.309	9.935(-1)	5.981(-1)	4.772(-1)
4	6.36 - 8.18	2.093	9.110(-1)	5.921(-1)	4.714(-1)
5	4.96 - 6.36	1.541	5.777(-1)	5.223(-1)	4.321(-1)
6	4.06 - 4.96	1.532	5.454(-1)	4.146(-1)	3.275(-1)
7	3.01 - 4.06	1.614	5.340(-1)	2.701(-1)	2.193(-1)
8	2.46 - 3.01	1.689	5.272(-1)	1.445(-1)	1.080(-1)
9	2.35 - 2.46	1.695	5.298(-1)	9.154(-2)	5.613(-2)
10	1.83 - 2.35	1.677	5.313(-1)	4.856(-2)	2.940(-2)
11	1.11 - 1.83	1.596	2.608(-1)	1.180(-2)	2.948(-3)
12	0.55 - 1.11	1.241	9.845(-3)	6.770(-4)	6.999(-5)
13	0.111 - 0.55	2.34(-1)	2.432(-4)	1.174(-6)	1.578(-8)
14	0.0033 - 0.111	6.928(-3)	3.616(-5)	1.023(-7)	1.389(-9)

[a] ENDF/B5 values that have been flux weighted (over CASK energy groups) based on a ^{235}U fission spectrum in the fast energy range plus a 1/E shape in the intermediate energy range.

APPENDIX F

References

[1] H. S. Palme, G. S. Carter, and C. L. Whitmarsh, Reactor Vessel Material Surveillance Program — Compliance With 10 CFR 50, Appendix H, for Oconee-Class Reactors, BAW-10100A, Babcock & Wilcox, Lynchburg, Virginia, February 1975.

[2] A. L. Lowe, Jr., K. E. Moore, and J. D. Aadland, Integrated Reactor Vessel Material Surveillance Program, BAW-1543, Babcock & Wilcox, Lynchburg, Virginia, November 1981.

[3] H. S. Palme and H. W. Behnke, Methods of Compliance With Fracture Toughness and Operational Requirements of Appendix G to 10 CFR 50, BAW-10046P, Babcock & Wilcox, Lynchburg, Virginia, October 1975.

[4] A. L. Lowe, et al., Irradiation-Induced Reduction in Charpy Upper Shelf Energy of Reactor Vessel Welds, BAW-1511P, Babcock & Wilcox, Lynchburg, Virginia, October 1980.

[5] DOT3.5 — Two-Dimensional Discrete Ordinates Radiation Transport Code (CCC-276), WANL-TME-1982, Oak Ridge National Laboratory, December 1969.

[6] CASK — 40-Group Coupled Neutron and Gamma-Ray Cross Section Data, RSIC-DLC-23, Radiation Shielding Information Center.

[7] C. L. Whitmarsh, Pressure Vessel Fluence Analysis, BAW-1485, Babcock & Wilcox, Lynchburg, Virginia, June 1978.